Paleoceanography and Paleoclimatology

RESEARCH ARTICLE
10.1029/2020PA003931

Mediterranean Overflow Over the Last 250 kyr: Freshwater Forcing From the Tropics to the Ice Sheets

Francisco J. Sierro[1], David A. Hodell[2], Nils Andersen[3], Lucia A. Azibeiro[1], Francisco J. Jimenez-Espejo[4,5], André Bahr[6], Jose Abel Flores[1], Blanca Ausin[1], Mike Rogerson[7], Rocio Lozano-Luz[8], Susana M. Lebreiro[8], and Francisco Javier Hernandez-Molina[9]

[1]Departamento de Geología, Universidad de Salamanca, Salamanca, Spain, [2]Department of Earth Sciences, University of Cambridge, Cambridge, UK, [3]Leibniz-Laboratory for Radiometric Dating and Isotope Research, Christian-Albrechts-Universität zu Kiel, Kiel, Germany, [4]Instituto Andaluz de Ciencias de la Tierra (CSIC-IACT), Granada, Spain, [5]Department of Biogeochemistry, JAMSTEC, Yokosuka, Japan, [6]Institute of Earth Sciences, Heidelberg University, Heidelberg, Germany, [7]School of Environmental Sciences, University of Hull, Hull, UK, [8]Instituto Geológico y Minero de España, Madrid, Spain, [9]Department of Earth Sciences, Royal Holloway, University of London, Egham, UK

Key Points:
- Mediterranean Overflow Water was governed by precession-driven freshwater forcing
- Ice sheets meltwater modified middepth Atlantic density and forced vertical changes in the settling depth of the MOW in the Atlantic
- Millennial-scale climate change interacted with precession to control the Mediterranean overflow during MIS 3 to 5

Supporting Information:
- Data Set S1

Correspondence to:
F. J. Sierro,
sierro@usal.es

Citation:
Sierro, F. J., Hodell, D. A., Andersen, N., Azibeiro, L. A., Jimenez-Espejo, F. J., Bahr, A., et al. (2020). Mediterranean overflow over the last 250 kyr: Freshwater forcing from the tropics to the ice sheets. *Paleoceanography and Paleoclimatology*, *35*, e2020PA003931. https://doi.org/10.1029/2020PA003931

Received 19 MAR 2020
Accepted 4 AUG 2020
Accepted article online 15 AUG 2020

Abstract To investigate past changes in the Mediterranean Overflow Water (MOW) to the Atlantic, we analyzed the strength of the MOW and benthic $\delta^{13}C$ along the last 250 kyr at Integrated Ocean Drilling Program (IODP) Site U1389 in the Gulf of Cadiz, near the Strait of Gibraltar. Both the strength of the MOW and the benthic $\delta^{13}C$ were mainly driven by precession-controlled fluctuations in the Mediterranean hydrologic budget. Reduced/enhanced Nile discharge and lower/higher Mediterranean annual rainfall at precession maxima/minima resulted in higher/lower MOW strengths at Gibraltar and stronger/weaker Mediterranean overturning circulation. At millennial scale, the higher heat and freshwater loss to the atmosphere during Greenland stadials increased buoyancy loss in the eastern Mediterranean. This enhanced the density gradient with Atlantic water, resulting in a higher MOW velocity in the Gulf of Cadiz. Unlike non-Heinrich stadials, a lower-amplitude increase in velocity was seen during Heinrich stadials (HSs), and a significant drop in velocity was recorded in the middle phase. This weak MOW was especially recognized in Termination I and II during HS1 and HS11. These lower velocities at the depth of Site U1389 were triggered by MOW deepening due to the lower densities of Atlantic intermediate water caused by freshwater released from the Laurentide and Eurasian ice sheets. The intrusion of salt and heat at deeper depths in the Atlantic during HSs and its shoaling at the end could have contributed to drive the changes in the Atlantic Meridional Overturning Circulation during Terminations.

Plain Language Summary The annual freshwater input to the Mediterranean from rivers and rainfall is lower than the water evaporated to the atmosphere each year. This annual water deficit generates an important outflow of salty water to the Atlantic. The Mediterranean Outflow circulates to the western Atlantic between 500 and 1,500 m, and the salt exported from the Mediterranean promotes the circulation of warm and salty water to the Norwegian sea. This heat circuit maintains relatively warm water in these latitudes. However, over the last 250 kyr, due to the heavy rainfall in tropical Africa, the Mediterranean water deficit decreased on various occasions. This reduced the export of salt to the Atlantic, causing changes in the Atlantic circulation. When the huge ice sheets that grew in Europe and North America started to vanish at the end of the last and penultimate glaciations, the meltwater released to the ocean decreased the salinity of the Norwegian, Greenland, and Labrador Seas. As a result, the density of intermediate waters reaching the Iberian Peninsula also decreased because they sink in these Nordic seas. The mixing of high-density Mediterranean water with low-density Atlantic intermediate water forced a deepening of the Mediterranean water in the Atlantic.

1. Introduction

The Mediterranean can be regarded as a thermodynamic machine driven by the combined action of a freshwater pump and a heat pump. Changes in the mode of operation of these two pumps determine Mediterranean thermohaline circulation through time and water exchange with the ocean (Bethoux &

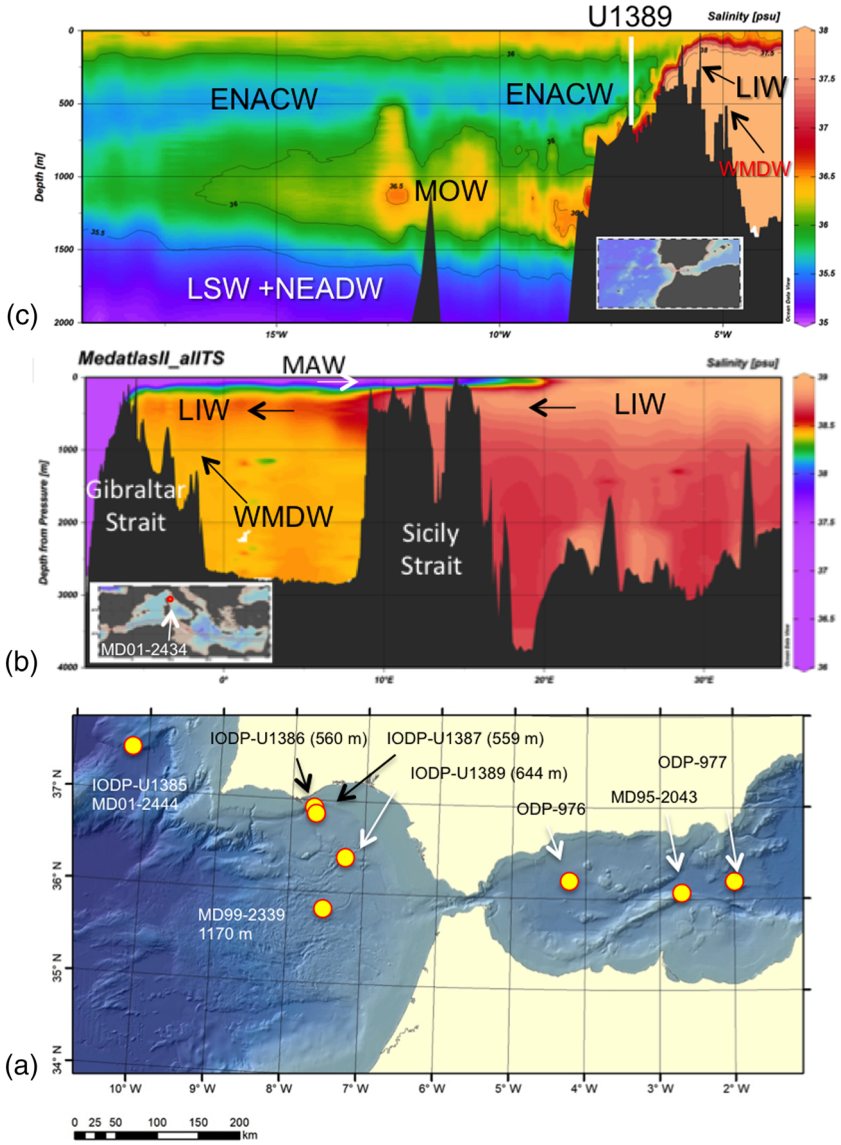

Figure 1. Location of the main cores mentioned in this study and hydrographic profiles of the NE Atlantic and Mediterranean. (a) Salinity profile of the northeastern Atlantic, the Strait of Gibraltar, and the westernmost Mediterranean, showing the main water masses in the Alboran Sea, the descending branch of the MOW, and the tongue of MOW in the Atlantic (World Ocean Database, WOD2018, Boyer et al., 2018). (b) Salinity profile showing the zonal Mediterranean overturning circulation formed by the eastward Atlantic inflow formed by the modified Atlantic water (MAW) and the westward Levantine intermediate water (LIW) (data from MedAtlas 2002-Database (Fichaut et al., 2003). (c) Map location of IODP Site U1389 in the Gulf of Cadiz as well as other sites referred to in this study. Legend for water masses (in alphabetic order): ENACW = east North Atlantic central water; LIW = Levantine intermediate water; LSW = Labrador Sea Water, MAW = modified Atlantic water, MOW = Mediterranean Overflow Water; NEADW = northeast Atlantic deep water, and WMDW = western Mediterranean deep water. The software Ocean Data View (Schlitzer, R., Ocean Data View, odv.awi.de, 2018) was used to generate the Atlantic and Mediterranean profiles.

Gentili, 1999; Bethoux et al., 1999; Millot et al., 2006; Skliris et al., 2007). Today, the MOW at Gibraltar is pumping water, heat, and salt to the Atlantic interior (Figures 1 and 2). It spreads between 500 and 1,500 m and can eventually reach the high latitudes of the North Atlantic (Bashmachnikov et al., 2015; Bryden & Stommel, 1984; Iorga & Lozier, 1999; Mauritzen et al., 2001; Ozgokmen et al., 2001; van Aken, 2000a). Any change in the physicochemical properties of this water mass in response to Mediterranean pumping of heat and salt may have an important impact on the vertical density gradient

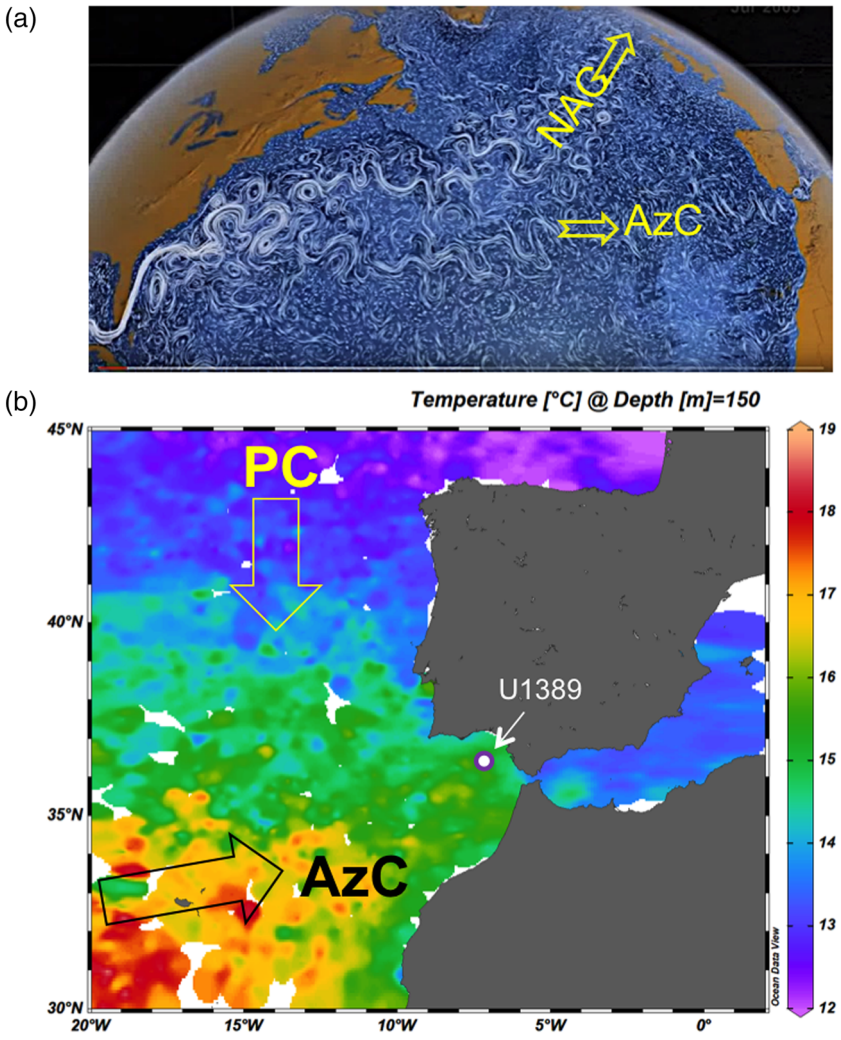

Figure 2. (a) Surface circulation in the North Atlantic, showing the Azores Current (AzC) and the North Atlantic Current (NAC) (image from video Perpetual Ocean, NASA Goddard). (b) February temperature at 150 m water depth offshore the Iberian Peninsula and the Gulf of Cadiz (World Ocean Database, WOD2018, Boyer et al., 2018) (The data set includes February temperature measurements from 1873 to 2017). We chose average February temperatures because they illustrate the heat transport from the AzC. The software Ocean Data View (Schlitzer, R., Ocean Data View, odv.awi.de, 2018) was used to generate this figure. Arrows indicate the Portugal Current and the AzC.

of the Atlantic and consequently on Atlantic Meridional Overturning Circulation (AMOC) and heat transport to the high latitudes (Bethoux et al., 1999; Ivanovic et al., 2014; Kida et al., 2008; Ozgokmen et al., 2001; Rahmstorf, 1998; Reid, 1979; Rogerson et al., 2006; Swingedouw et al., 2019). On the other hand, changes in the AMOC and the physical properties of the Atlantic intermediate and deep water masses could also affect the MOW settling depth in the Atlantic.

Past changes in the export of salt and heat to the global ocean were mainly driven by variations in water exchange at Gibraltar that were, in turn, controlled by the geometry of the strait and the density difference between the inflowing and outflowing waters (Bethoux, 1979; Bryden et al., 1994). Modeling studies have explored the response of the MOW to several oceanographic parameters such as sea level or changes in the net evaporative flux of the Mediterranean as well as changes in the vertical density gradient of Atlantic water masses (Rogerson, Rohling, et al., 2012).

Because of the net loss of water in the Mediterranean (evaporation exceeding precipitation plus runoff) and the cold winds reaching the northern margins of the basin the density of Mediterranean water at Gibraltar is much higher than that of the Atlantic surface water, resulting in a Mediterranean Outflow at depth and an

Atlantic inflow at surface (Bethoux & Gentili, 1999; Bryden et al., 1994). A series of studies have investigated the evolution of the MOW by analyzing changes in the physical or geochemical properties of the sediments in various sites along the Gulf of Cadiz contourite depositional system (Bahr et al., 2015; Bryden & Kinder, 1991; Bryden & Stommel, 1982; Kaboth et al., 2016; Kaboth, de Boer, et al., 2017; Kaboth, Grunert, et al., 2017; Kaboth-Bahr et al., 2018; Lebreiro et al., 2015, 2018; Llave et al., 2006; Singh et al., 2015; Stow et al., 2013; Toucanne et al., 2007; Voelker et al., 2006, 2015). Most of them point to the straight relationship between the intensity of MOW and Northern Hemisphere climate variability. The longer records suggest a strong correlation with orbital changes in African monsoons (Bahr et al., 2015; Kaboth et al., 2017; Kaboth-Bahr et al., 2018; Lofi et al., 2016; Voelker et al., 2015). However, there are still some features of the MOW variability, that remain poorly understood, especially those associated to MOW behavior during Heinrich stadials (HSs) and the interaction between orbital and millennial-scale variability because most of the works already published about the millennial response of the MOW are focused on the last 60 kyr, where the influence of precession is small. In addition, most studies were more focused on the variability of MOW strength, but changes in its chemical properties are less known.

In this study, we analyze and discuss the evolution of the chemical and physical properties of the MOW and the main mechanisms that have governed its evolution along the last 250 kyr through a detailed analysis of Site U1389 drilled during Integrated Ocean Drilling Program (IODP) expedition 339 in the Gulf of Cadiz. We compare the precession-driven changes in MOW strength triggered by Mediterranean freshwater forcing, with the millennial-scale response of the MOW during Marine Isotope Stage (MIS) 5 and explore the impact of freshwater release from the European and Laurentide ice sheets on the settling depth of the MOW in the Atlantic.

We will address first the orbital-scale MOW variability along the last 250 kyr to continue with a more detailed analysis of millennial-scale variability during HS1 and the Holocene, MIS 3 to 5 and Termination II.

2. MOW and NE Atlantic Circulation Today

Mediterranean overturning circulation is driven by dense water formation in the northern margins of the Mediterranean and is regulated by heat and freshwater atmospheric forcing due to heat and freshwater exchange with the atmosphere during winter (Jorda, Sanchez-Roman, et al., 2017; Jorda, Von Schuckmann, et al., 2017; Pinardi & Masetti, 2000). The Gulf of Lion-Ligurian seas are the areas of western Mediterranean deep water (WMDW) formation (Millot, 1999; Schott et al., 1996; Schroeder et al., 2008), while surface water from the Adriatic, Aegean and Levantine seas sink to form the eastern Mediterranean deep and intermediate water (Kubin et al., 2019; Lascaratos et al., 1993; Roether & Schlitzer, 1991; Roether et al., 1996; Tsimplis & Bryden, 2000).

The inflow-outflow currents at Gibraltar are mainly linked to the zonal overturning circulation formed by the Atlantic water moving eastward at the surface and the Levantine intermediate water (LIW) moving westward between 150 and 500 m depth, being the main component of the outflow at Gibraltar with a small contribution of the WMDW (Millot, 1999, 2013; Pinardi et al., 2019) (Figure 1).

Dense water formation, is highly dependent on salt preconditioning that is governed by the Mediterranean freshwater budget. Winters with persistent cool and strong northerlies will cause significant heat loss. As a result, a large volume of new, dense water is introduced in the Mediterranean interior, contributing to its ventilation and to increase the MOW density at Gibraltar (Bethoux & Gentili, 1999; Bethoux & Pierre, 1999; Criado-Aldeanueva et al., 2012; Jorda, Sanchez-Roman, et al., 2017; Josey, 2003; Millot, 1999). However, rivers from the northern Mediterranean catchment areas, such as the Rhone in the Gulf of Lion, the Po in the Adriatic or the Black Sea and the Nile in the Levantine basin will deliver freshwater to the sea basins, lowering sea surface salinity in the source areas of deep or intermediate water formation. These freshwater discharges tend to reduce the rates of dense water formation with final implications in the velocity of the MOW at Gibraltar (Bethoux & Gentili, 1999; Bethoux & Pierre, 1999; Criado-Aldeanueva et al., 2012; Josey, 2003; Skliris et al., 2007).

The MOW at the exit of the Strait of Gibraltar is a salty, high-density current formed by a mixture of LIW and WMDW with an average salinity and temperature of 38.4 psu and 13°C, respectively (Figure 1) (Bryden & Stommel, 1982; Garcia-Lafuente et al., 2017; Gasser et al., 2017; Hernández-Molina et al., 2014;

Millot, 2014; Sanchez-Leal et al., 2017). After crossing the Camarinal Sill in the Strait of Gibraltar, at 290 m water depth, this dense MOW cascades down into the Gulf of Cadiz, as an overflow (Legg et al., 2009), accelerating because of its density anomaly and mixes and entrains the overlying fresher eastern North Atlantic central water (ENACW). Because of this mixing, the MOW reduces its salinity and temperature to transform into the MOW that settled within the Atlantic between 500 and 1,500 m (Figure 1) (Ambar & Howe, 1979; Baringer & Price, 1997; Bashmachnikov et al., 2015; Sanchez-Leal et al., 2017; van Aken, 2001). Most of this mixing and entrainment occurs within the first 100 km along the MOW path after the Strait of Gibraltar and as a result the MOW volume transport increases from 0.8 Sv at the strait to more than 2.7 Sv when the MOW reaches its equilibrium depth in the Atlantic (Baringer & Price, 1997; Legg et al., 2009; Sanchez-Leal et al., 2017). During its descent the MOW splits in two cores, the upper one that mixes with the warmer upper waters of the ENACW settle in the Atlantic at a few hundred meters (300–800 m) because of its higher temperatures. In contrast, the lower core settles in the Atlantic at a deeper depth (1,100 to 1,500 m) as it reaches a higher density because of the mixing with and entrainment of a deeper and colder section of the ENACW (Baringer & Price, 1997; Gasser et al., 2017; Hernández-Molina et al., 2014; Sanchez-Leal et al., 2017). This lower core has a slightly different salinity than the upper core but a much colder temperature. The speed of the MOW gradually decreases from up to 300 cm s^{-1} at the Strait of Gibraltar to around 15–20 cm s^{-1} in Cape Saint Vincent (Ambar & Howe, 1979; Gasser et al., 2017; Price et al., 1993; Sanchez-Leal et al., 2017). As a result, sediments at the seafloor were profoundly affected by these bottom currents to form a huge contourite depositional system along the southern and west Iberian Margin (Faugeres et al., 1984; Hernández-Molina et al., 2003, 2014, 2016; Llave et al., 2007; Nelson et al., 1993; Stow et al., 1986).

Surface circulation along the southwest Iberian Margin is mainly driven by eastward advection of subtropical salty water of the Azores Current (AzC) and the southward advection of the less salty and cooler water of the Portugal Current. The convergence of these water masses forms the subtropical front offshore southern Portugal (Peliz et al., 2005) (Figure 2). The Atlantic inflow into the Mediterranean is mainly composed of waters fed from AzC (Peliz et al., 2009; Soto-Navarro et al., 2012).

MOW mixes in the Atlantic with different water masses (Bashmachnikov et al., 2015; Carracedo et al., 2015, 2016; Roque et al., 2019) (Figure 1). The ENACW that flows between 400 and 700 m over the MOW is composed by the upper ENACW formed in the subtropical region near the Azores front, and the deep ENACW, also referred to as the polar ENACW, formed by winter cooling in the bay of Biscay (Bashmachnikov et al., 2015; Carracedo et al., 2015; Roque et al., 2019; van Aken, 2001) (Figure 1a). The upper ENACW and deep ENACW are the subsurface components of the AzC and the Portugal Current, respectively. More to the south, the MOW mixes with Antarctic intermediate water (AAIW), which flows northward along the Moroccan margin toward the Gulf of Cadiz between 600 and 1,000 m deep (Bashmachnikov et al., 2015; Carracedo et al., 2015; Roque et al., 2019; van Aken, 2000; Voelker, Colman, et al., 2015).

Underlying the MOW, the Labrador Sea Water (LSW) and the northeast Atlantic deep water (NEADW) (Figure 1a), which are formed by water masses originated from the Labrador, Iceland, and Scotland seas in the subpolar region, move deeper than 1,500 m. The density of LSW and NEADW is very similar to that of the MOW (Bashmachnikov et al., 2015; Carracedo et al., 2015).

3. Materials and Methods

3.1. Site U1389

IODP Site U1389 is located in the Gulf of Cadiz (36°25.515′N; 7°16.683′W) at a water depth of 644 m and a distance of 100 km from the Strait of Gibraltar (Figure 1c). It was drilled in the Huelva sheeted drift developed along the middle slope under the influence of the main descending branch of the MOW. Bottom water salinities around 37 psu indicate the presence of MOW still not fully mixed with the ENACW (Sanchez-Leal et al., 2017). In consequence, past physicochemical properties at this site would reflect better the original properties of the MOW than the more distal sites. Because Site U1389 was drilled in the middle of the Huelva sheeted drift, which is surrounded by contourite channels, the source of sediment is mainly pelagic or transported/reworked by the MOW (de Castro et al., 2020). We sampled the upper 130 m along the splice with a resolution of 10 cm. A succession of mud and sandy silty contourite beds were observed in this

interval (Stow et al., 2013). Approximately 20 cc of sediment were freeze dried overnight, weighed, disaggregated in tap water and poured into a 62 μm sieve to remove the fine sediment and this residue was dried and dry sieved again using a 150 μm sieve.

3.2. Fine Sand Percentage and Coarse Sand/Total Sand Ratio

To calculate the fine sand content, we used the weight percent of the 63–150 μm fraction relative to the dry bulk sediment. We also estimated the coarse sand/total sand ratio which is the weight% of the fraction >150 μm/(weight% of the fraction 62–150 μm + weight% of the fraction >150 μm). The fraction >150 μm is mainly dominated by planktonic foraminifers. Note that the sand fraction includes biogenic and detrital sand. We also calculated the concentration of coccoliths per gram in the sediment following the method of Flores and Sierro (1997).

3.3. Ice-Rafted Debris

Detrital particles are abundant in the fraction 62–150 μm, however, with the exception of some micas they are absent in the sand fraction. To explore the potential presence of ice-rafted debris (IRD), we counted the lithic grains larger than 250 μm for the interval corresponding to HS1.

3.4. Stable Isotopes

Approximately 30 specimens of *Globigerina bulloides* from the 250 to 300 μm size fraction and 2–10 individuals of *Cibicidoides pachyderma* larger than 250 μm were picked to measure oxygen and carbon isotope ratios. Foraminifer tests were soaked in 15% H_2O_2 to remove organic matter, and cleaned sonically in methanol to remove fine-grained particles. Samples of *Cibicidoides* from 0 to 29.38 mcd were measured in the Godwin Laboratory for Paleoclimate Research at the University of Cambridge. The rest of the samples were measured at the Laboratory for Isotope Research at the Christian-Albrecht University in Kiel. All samples were measured with a Thermo Finnigan MAT 253 mass spectrometer connected to a Kiel IV carbonate preparation device. The analytical precision of the NBS-19 international standard and three laboratory internal standards was better than ±0.05‰ for $\delta^{13}C$ and ±0.08‰ for $\delta^{18}O$. At the Christian-Albrecht University, large foraminiferal samples with more than six individuals were crushed to homogenize the samples before analysis of a representative subsample was undertaken. Results are reported relative to the Vienna Pee Dee Belemnite standard.

To estimate the $\delta^{18}O$ of surface seawater at Site U1389, we first calculate the seasurface temperature using the neural networks method based on the planktonic foraminifer assemblages. Then the *G. bulloides* $\delta^{18}O$ was corrected for the sea surface temperature (SST) effect.

4. Results and Discussion

4.1. Age Model

For the last 120 kyr, the chronology for IODP Site U1389 was established through synchronization of the *G. bulloides* $\delta^{18}O$ record to Greenland $\delta^{18}O$ ice core record using the Greenland GICC05 chronology (Rasmussen et al., 2014). For older ages we synchronized the *G. bulloides* $\delta^{18}O$ record to Greenland synthetic record using the absolute chronology of Asian speleothem records based on uranium series datings (Barker et al., 2011) (Figure 3). For some specific events, such as onset and end of HSs at the end of MIS 6 and MIS 8, which are clearly defined in the Asian speleothem records and are not well expressed in the Greenland synthetic reocord, we used the chronology of Cheng et al. (2016). Our *G. bulloides* $\delta^{18}O$ record was also correlated with that of MD01-2444/2443 (Hodell et al., 2013; Martrat et al., 2007) in the Portuguese margin that was also synchronized with the Greenland synthetic record (Barker et al., 2011). The depth-age points used to build the chronology of Site U1389 is shown in Table 1.

4.2. Bottom Current Strength at Site U1389

The Gulf of Cadiz has been a natural laboratory for the study of contourite sediments (Faugeres et al., 1984; Gonthier et al., 1984; Llave et al., 2001; Stow et al., 1986, 2002). Grain size in contourite deposits depends on the size of the particles supplied by rivers or from downslope transport, the size of settling biogenic particles and the velocity of bottom currents (Faugeres et al., 1984; Mulder et al., 2013; Stow et al., 1986). At Site U1389 the vigor of bottom currents is so high that grain size is mainly controlled by changes in velocity through time (de Castro et al., 2020; Stow et al., 1986). Besides the mean grain size of the detrital fraction

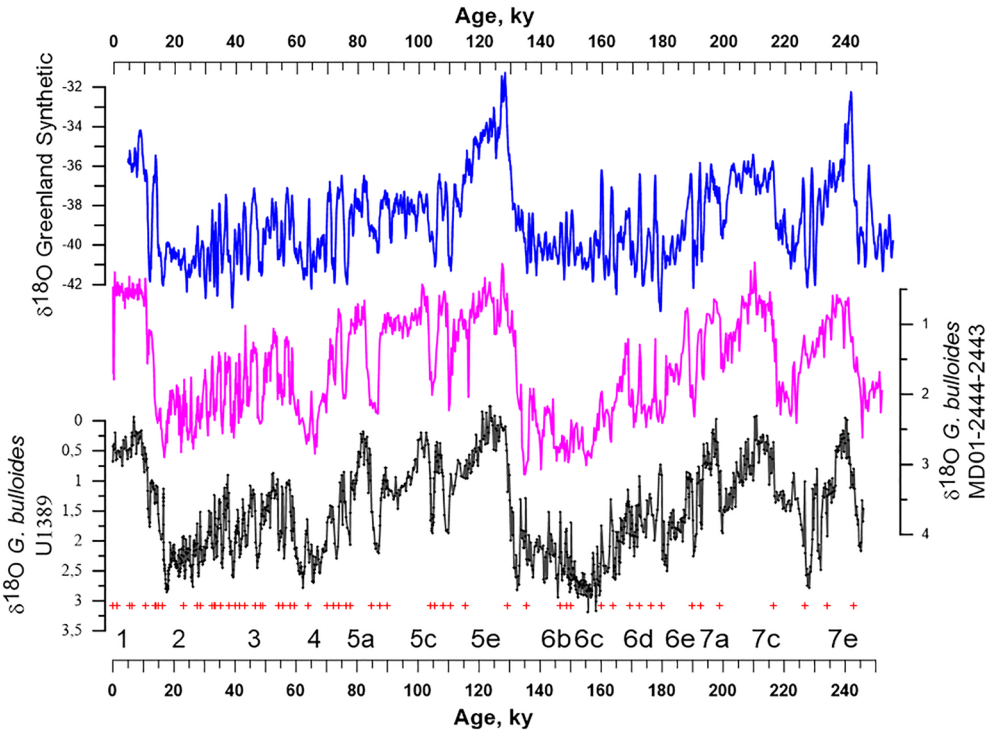

Figure 3. Chronologic framework for U1389. Red crosses are the tie points (see Table 1) used for tuning U1389 with Greenland ice cores and Greenland Synthetic record as well as the events aligned with the $\delta^{18}O$ of Asian speleothem records (Cheng et al., 2016) (see Table 1). (bottom) $\delta^{18}O$vpdb of *G. bulloides* from IODP Site U1389 (black). (middle) $\delta^{18}O$vpdb of *G. bulloides* from the combined record of MD01-2444 and MD01-2443 (magenta) (Hodell et al., 2013; Martrat et al., 2007). (top) Greenland synthetic $\delta^{18}O$ record (blue) (Barker et al., 2011). Code numbers at the bottom denote MIS stages and substages after Railsback et al. (2015).

10–62 μm, also known as the sortable silt fraction (McCave et al., 1995), other proxies such as median grain size or the percentage of sand (fraction higher than 62 μm, including carbonate or carbonate-free particles) have been used to track past changes in bottom water velocities in the Gulf of Cadiz (Brackenridge et al., 2018; Lebreiro et al., 2018; Llave et al., 2006; Mulder et al., 2013; Toucanne et al., 2007; Voelker et al., 2006). In this study we used the percentage of fine sand (fraction 62–150 μm) (including detrital and biogenic particles) as a proxy for the strength of the MOW at Site U1389 along the last 250 kyr (Figure 4). The higher content of fine sand is due to the action of bottom currents combined with the activity of macrobenthic organisms that continuously bioturbate and resuspend the sediments, resulting in the winnowing of fine-grained particles, mainly detrital clay and silts as well as coccoliths and other fine-grained biogenic material (Brackenridge et al., 2018; Sierro et al., 1999; Stow et al., 1986). This process is also favored by the long time the particles spend in the mixed layer before burial because of the low sedimentation rates in some of the sandy contourite beds (Sierro et al., 1999). As a result, sand particles are concentrated in the sediments. We excluded the coarse sand (fraction >150 μm) because it is mainly dominated by biogenic carbonate shells with almost no detrital grains. The main component of the coarse-sand fraction are planktonic foraminifers, with a small proportion of fragments of gastropods, bivalves, echinoderm spines and ostracods. In consequence, changes in the percentage of this size fraction may be affected by biogenic productivity besides lateral transport. By contrast, fine sand is dominated by detrital particles that may reach more than 90% of the fine sand fraction in the more sandy intervals, although biogenic carbonate tests are also abundant. The content of sand particles in the sediment also depends on sediment input from the continent and downslope transport, but the impact of the bottom currents is so intense that changes in continental input are minimized. In consequence, we assumed that the percentage of fine sand can be used as a proxy for the velocity of the MOW.

Table 1
Depth-Age Tie Points Used to Build the Chronology of Site U1389

Depth (mcd)	Age	Events	Radiocarbon age (yr)
0	0		
0.82	1.24	(AMS 14C)	1930 ± 30 BP
2.02	5.6	(AMS 14C)	5480 ± 40 BP
2.32	6.26	(AMS 14C)	6070 ± 40 BP
4.24	10.71	(AMS 14C)	9980 ± 50 BP
6.44	13.86	(AMS 14C)	12640 ± 50 BP
6.64	14.3345	(AMS 14C)	12950 ± 40 BP
6.94	14.802	(AMS 14C)	13330 ± 40 BP
7.24	16.37	(AMS 14C)	14030 ± 60 BP
14.12	23.02	GI2.1	
14.62	23.34	Bottom GI2.2	
18.17	27.73	Bottom GI3	
18.98	28.85	Bottom GI4	
20.98	32.45	Bottom GI5	
21.35	33.31	Top GI6	
21.79	33.69	Bottom GI6	
23.4	35.43	Bottom GI7	
25.91	38.17	Bottom GI8	
26.96	40.16	Bottom GI9	
28.57	41.41	Bottom GI10	
29.92	43.29	Bottom GI11	
31.63	46.81	Bottom GI12	
32.53	48.29	Top GI13	
33.44	49.23	Bottom GI13	
36.46	54.17	Bottom GI14	
37.12	55.75	Bottom GI15	
38.32	58.23	Bottom GI16	
39.34	59.44	Bottom GI17.2	
41.85	64.1	Bottom GI18	
44.32	70.23	Top GI19	
44.92	72.34	Bottom GI19.2	
45.32	74.2	Top GI20	
46.25	76.44	Bottom GI20.c	
46.56	77.8	Top GI21	
50.27	84.76	Bottom GI21.1e	
51.28	87.6	Top GI22	
52.1	90.04	Bottom GI22.g	
56.35	104.04	Bottom GI23.1	
57.61	105.4	Top GI24	
59.84	108.28	Bottom GI24.2	
60.44	110.8	GI25a	
61.26	115.37	Bottom GI25	
66.41	129.43	Top HS11 (age Cheng et al., 2016)	
68.77	135.60	Bottom HS11 (age Cheng et al., 2016)	
72.89	146.62	Warming in MIS 6b	
74.3	148.55	Warming in MIS 6b	
76.03	150.26	Warming in MIS 6b	
83.59	160.08	Warming in MIS 6d	
84.62	163.91	Warming in MIS 6d	
88.92	169.31	Warming in MIS 6d	
91.3	172.70	Warming in MIS 6d	
92.26	176.21	Warming in MIS 6d	
93.06	179.90	Warming bottom MIS 6d	
98.61	189.87	Warming in MIS 6e	
99.77	192.57	Warming in MIS 6e	
103.31	198.88	Bottom warming MIS 7a	
109.65	216.5	Bottom MIS 7c	
112.26	226.75	Warming event in MIS 7d	
115.33	234.18	Abrupt cooling in MIS 7d	

Table 1
Continued

Depth (mcd)	Age	Events	Radiocarbon age (yr)
119.75	242.67	Bottom MIS 7e	
130	263.83	Top Heinrich (age Cheng et al., 2016)	

In addition, we also estimated the ratio of coarse sand/total sand (Figure 5). This ratio changed from 0 (no coarse sand >150 μm) to 1 (all sand particles are larger than 150 μm). It reached the highest values at times of the slowest MOW because the accumulation of pelagic shells (concentrated in the coarse sand) dominates over deposition of fine sand particles transported by bottom currents. In contrast, intense MOW will result in the accumulation of fine sand transported by bottom currents in detriment of pelagic foraminifers (Figure 5a).

Both the record of fine sand and the coarse sand/total sand ratio at Site U1389 (Figures 4b and 5a) show high amplitude changes that are correlated with the interbedding of sandy contourite layers and mud beds. The fine sand content at Site U1389 today is relatively high due to the high speed of the MOW flowing over this site, which is in the order 0.1–0.5 m s^{-1} (Sanchez-Leal et al., 2017). The overall good correlation between the record of fine sand content and the Zr/Al record published by (Bahr et al., 2015; Kaboth-Bahr et al., 2018) (Figure 4c) support that the fine sand percentage used in this study is a good proxy for the strength of the MOW at this site. The high abundance of detrital particles, including heavy minerals, in the fine sand fraction (Bahr et al., 2015) explains this correlation and supports the existence of a high-velocity bottom current capable of transporting fine sand detrital particles along the slope of the Gulf of Cadiz. Removal of fine-grained particles by winnowing due to this high-speed current was behind the generation of these sandy-rich contourite beds as reported by various authors (Gonthier et al., 1984; Stow et al., 1986).

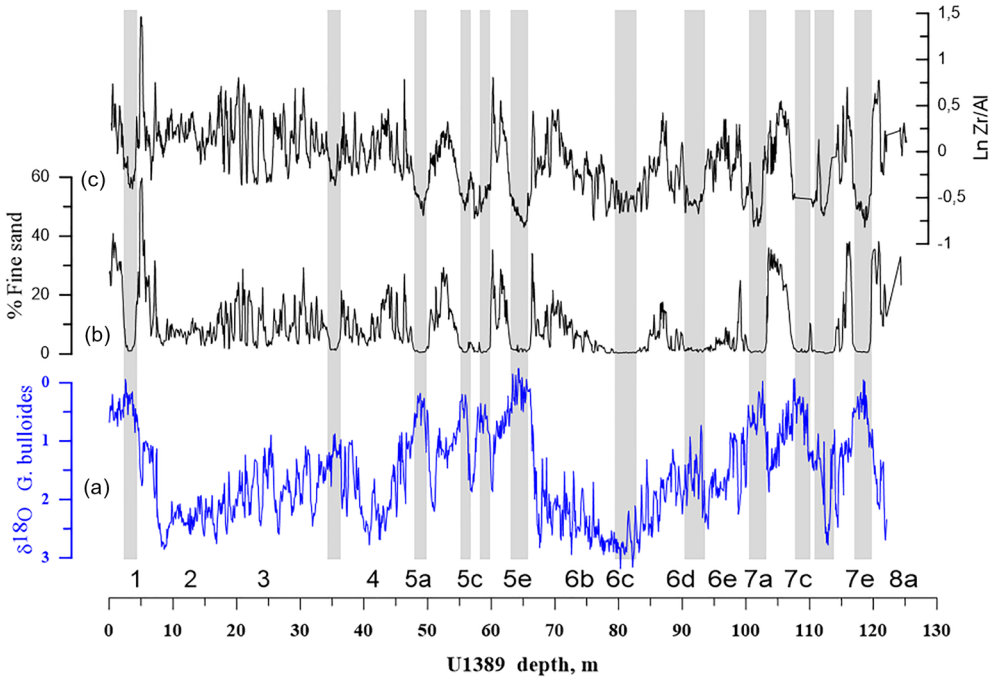

Figure 4. Change in strength of the MOW along the last 250 kyr at IODP Site U1389. (a) IODP Site U1389 *Globigerina bulloides* $\delta^{18}O$ record. (b) Percent fine sand (fraction 62–150 μm). (c) Zr/Al record (Bahr et al., 2015; Kaboth-Bahr et al., 2018). Codes at the bottom show MIS stages and substages after Railsback et al. (2015). Gray vertical bars show the intervals with very weak MOW (minimum percent of fine sand).

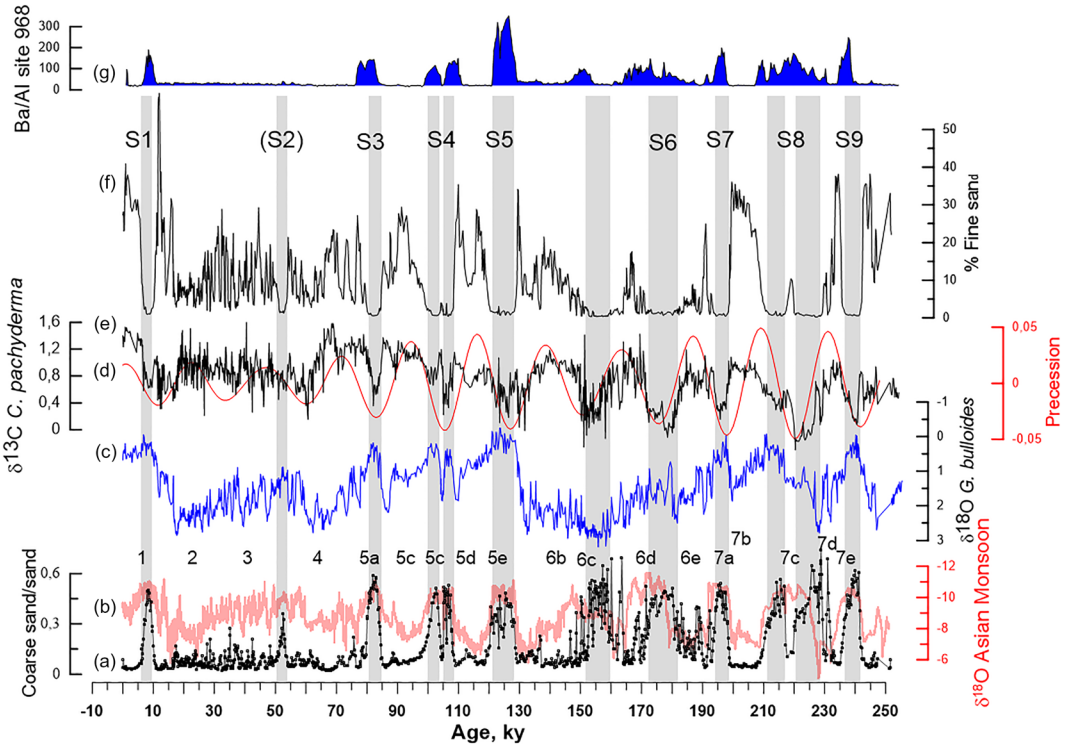

Figure 5. Correlation between events of reduced MOW strength at Site U1389, eastern Mediterranean stagnation events (sapropels), weak Mediterranean thermohaline circulation, and episodes of Asian Monsoon intensification. (a) Ratio of coarse sand/total sand (fraction >150 μm)/total sand. (b) $\delta^{18}O$ from Asian speleothems (Cheng et al., 2016). (c) *G. bulloides* $\delta^{18}O$ at Site U1389. (d) Precession index. (e) *Cibicidoides pachyderma* $\delta^{13}C$ at Site U1389. (f) Percent fine sand (fraction 62–150 μm) at Site U1389. (g) Ba/Al ratio at ODP Site 968 in the eastern Mediterranean (Ziegler et al., 2008). Gray bands indicate periods of weak MOW at the Strait of Gibraltar (lowest fine sand percentages). S1 to S9 denote Sapropels. MIS stages and substages after Railsback et al. (2015) are shown below the *G. bulloides* $\delta^{18}O$ record.

5. MOW Strength, Mediterranean Overturning, and Sapropels Over the Last 250 kyr

Although MOW velocity at a single site can be affected by changes in its settling depth (Rogerson, Rohling, et al., 2012), the proximity of Site U1389 to the Strait of Gibraltar, its location near the main descending core of the MOW and its salinity of 37 psu (Sanchez-Leal et al., 2017) indicate that bottom water at this site today is a relatively pure MOW, still not well mixed with the colder and less saline ENACW. All this minimizes the impact of the MOW settling behavior after its exit at the Camarinal Sill. Comparing MOW strength records of the more distal sites U1386 and U1387 with those of Site U1389, Bahr et al. (2015) concluded that the velocity patterns in the last site mainly reflect variations in MOW strength in the Strait of Gibraltar. In addition, changes in strength observed in this study are very similar to those recorded in the deeper core MD99-2339 (Voelker et al., 2006) (1,170 m depth), supporting again that changes in MOW velocity at these different depths were mainly driven by MOW behavior in the Strait of Gibraltar. This does not exclude that some of the changes in MOW strength recorded at Site U1389 have been weakly affected by deepening or shallowing of the MOW as discussed below.

The percentage of fine sand in the sediments changed from near 0% to 60% along the last 250 kyr (Figure 4b). Periods of strong bottom water velocity alternate with times of quiet MOW. The similarity between the MOW strength patterns seen at Site U1389 for the last 140 kyr and changes in LIW velocity in the Corsica margin (Toucanne et al., 2012) confirms that the MOW velocity at Site U1389 is mainly controlled by changes in the Mediterranean heat and freshwater budgets. In particular we identified 10 beds (some of them are double beds) with almost no fine sand (Figure 5f). These beds are linked to times of very weak MOW in the Gulf of Cadiz and are characterized by sand contents lower than 2% and a distinct high

coarse sand/total sand ratio (Figure 5a) due to the high percentages of planktic foraminifers, mostly reflecting a hemipelagic settling. These prominent minima in fine sand content are related to minima in the planktic $\delta^{18}O$ record during MIS 1, 5a, 5c, 5e, MIS 6c, d, and MIS 7a, 7c, 7e (Figures 4 and 5).

While the velocity of the MOW is recorded by changes in the percentage of fine sand, its chemical properties can be characterized by the benthic $\delta^{13}C$ at Site U1389, which mainly reflects the Mediterranean $\delta^{13}C$ signature partially modified during mixing with Atlantic water at Gibraltar. The Mediterranean $\delta^{13}C$ signature is, in turn, the result of the $\delta^{13}C$ of surface waters in the source of intermediate water formation and Mediterranean overturning circulation, which tends to reduce the $\delta^{13}C$ of the MOW dissolved inorgancic carbon as Mediterranean overturning weakens.

The overal good correlation between the benthic $\delta^{13}C$ at Site U1389 and the percentage of fine sand or coarse sand/total sand (Figure 5) confirms that MOW strength variability mainly reflects past changes of Mediterranean overturning circulation. Times with higher fine sand contents in the sediment usually show high benthic $\delta^{13}C$ values, whereas periods with low fine sand concentrations display lower benthic $\delta^{13}C$.

As seen in Figure 5, the $\delta^{13}C$ of the MOW follows Earth's precession, showing depleted ^{13}C during precession minima (Northern Hemisphere summer insolation maxima) and high $\delta^{13}C$ at precession maxima (Northern Hemisphere summer insolation minima). The small offsets between the lowest benthic $\delta^{13}C$ and insolation maxima, especially during MIS 6, are due to the different age scales used at Site U1389 and ODP Site 968. We used the Greenland chronology and sapropels of Site 968 were tuned to insolation (Ziegler et al., 2010). Therefore we can conclude that benthic $\delta^{13}C$ at site u1389 is recording the precession-driven changes of Mediterranean overturning circulation with poor ventilation at times of precession minima and higher rates of intermediate water ventilation at precession maxima.

In particular the 10 beds that display the lowest fine sand contents at times of precession minima are characterized by pronounced drops of the benthic $\delta^{13}C$ record (Figure 5e). This points to a strong connection between the events of MOW colapse at Gibraltar, reduced Mediterranean ventilation and higher rates of carbon remineralization at times of precession minima. In consequence, we conclude that the periods with very low benthic $\delta^{13}C$ and collapse of the MOW at Gibraltar registered the times of sapropel deposition in the eastern Mediterranean as reported by (Bahr et al., 2015; Kaboth et al., 2017). The close coherence of the fine sand content at site u1389 and the Ba/Al ratio in sediments from the deep eastern Mediterranean, which records higher biogenic barite contents, confirms the strong coupling between weak MOW at Gibraltar and Mediterranean sapropels (Ziegler et al., 2010) (Figures 5e and 5f).

Northward latitudinal migrations of the Intertropical Convergence Zone (ITCZ) and intense monsoons in Africa and Asia have been related to large summer Nile discharges (Castañeda et al., 2016; Revel et al., 2010) and sapropel formation (Rohling & Hilgen, 1991; Rohling et al., 2015; Rossignol-Strick et al., 1982). Events of enhanced Nile discharge were also synchronous to periods of increase annual rainfall in the northern and southern Mediterranean catchment areas (Bar-Matthews et al., 2000; Toucanne, Minto'o, et al., 2015; Tzedakis, 2005; Tzedakis et al., 2002, 2009; Wagner et al., 2019; Zanchetta et al., 2007), showing the strong coupling between the low and midlatitude hydrological cycle (Bosmans et al., 2015, 2020; Kutzbach et al., 2014; Marzocchi et al., 2019). Our data thus confirms the strong link between precession minima, instense Asian and African monsoons, sapropels and weak MOW at Gibraltar. This finding is significant, because it further links low-latitude changes in precipitation to high latitude seawater density.

Nonetheless, rainfall in the tropics occurred in summer, while Mediterranean precipitation probably took place in winter and fall based on pollen records from the Balkans (Tzedakis, 2005; Tzedakis et al., 2009). Regardless of its seasonal origin, this freshwater forcing reduced sea surface salinity and density and prevented intermediate and deep water formation. The low rates of LIW production reduced the density anomaly and the intensity of the MOW at Gibraltar and therefore the strength of the MOW at Site U1389. The higher winter SST due to lower heat loss in the eastern Mediterranean during milder winters could also further reduce the vertical density gradient, contributing to increase water stratification and reduce the annual rates of LIW formation. This lower Mediterranean heat loss is expected because northern Europe was less covered by snow at times of precession minima, especially at times of reduced ice sheet extension and therefore winter air temperature in the Gulf of Lion, the Adriatic and Aegean seas. Pollen records from Southern Europe and Anatolia show that large expansions of the temperate forest are closely associated to

insolation (Litt et al., 2014; Magri & Tzedakis, 2000; Tzedakis et al., 2006, 2009). In consequence, at times of precession minima both the freshwater and heat pumps were working together to decrease the densification of Mediterranean waters.

The sensitivity of MOW strength at site u1389 to changes of Mediterranean freshwater forcing is so high that the time of maximum insolation at around 155 kyr that did not leave any sapropel in the eastern Mediterranean is well expressed in our site by a very weak MOW. However, the weak MOW recorded at this time is also linked to an important meltwater event in the Fennoscandian ice sheets (Boswell et al., 2019; Toucanne, Minto'o, et al., 2015) resulting in IRD deposition (Barker et al., 2015) and a change of the hydrography of deep and intermediate water circulation in the North Atlantic. See sections 7.1 and 8 for a discussion about MOW deepening during HSs.

One period of low MOW flow, during MIS 3 (Figure 5), is related to Sapropel S2, which is rarely expressed in the eastern Mediterranean. This period does not correspond to a peak in Ba/Al in the eastern Mediterranean, although it does date to the time of an important decrease of benthic $\delta^{13}C$ in core MD04-2722 related with reduced eastern Mediterranean deep water ventilation (Cornuault et al., 2016). However, the pronounced drop in fine sand and an increase in the coarse sand/total sand record (Figure 5) indicates that Mediterranean density was profoundly reduced at this time in a manner comparable to "true" sapropels. This event is also recorded as one of the most wet phases of north African climate in Libyan speleothems (Hoffmann et al., 2016). This period stands out within the record, as the phasing with respect to precession is different to other periods of low MOW flow. The onset of this low flow period is delayed by about 10 kyr compared to other events. Hoffmann et al. (2016) also found this wet period did not relate to precession but rather to obliquity. This obliquity-forced decline in Mediterranean density seems to be unique within the last 250 kyr (Figure 5). It is further suggestive that this period had different forcing to precession-related peaks in humidity because the two precession peaks within MIS 3 do not have minima in MOW flow (Figure 5). These precession-forced periods in MIS 3 also have rainfall moisture with a significant component from within the Mediterranean according to speleothem fluid inclusion analysis, unlike the obliquity-forced phase (Rogerson et al., 2019).

6. MOW Strength During Termination I and the Holocene

Over the last 20 kyr, three distinct sandy contourite beds were recognized at Site U1389 (Figures 6 and 7). They have been widely recognized throughout the Gulf of Cadiz as sandy contourite Layers I, II, and III (Stow et al., 1986). These sandy contourites (SC) were deposited during the Late Holocene (SCIII), Younger Dryas (SC II) and latest part of HS1 (SC I) (Figure 6). The minimum concentration of Coccoliths/g in these layers confirms the impact of bottom waters at those times through winnowing of fine-grained particles. However, the muddy interval between SC III and SCII characterized by low percentages of fine sand and an anomalously high coarse sand/total sand ratio (Figure 5a) indicates that sediment accumulation during this period was mainly driven by settling of pelagic particles, such as planktic foraminifera and coccoliths (Figures 5a and 6) and low proportions of detrital particles. All this indicates there was no impact of bottom current activity during the early Holocene (Figure 6). This prominent MOW velocity miminum during the early Holocene, which is also seen at deeper water depths (Voelker et al., 2006), is a widespread feature that has already been recognized as the "Holocene contourite gap" (Stow et al., 1986), and to date appears to be common to every core recovered from this margin (Llave et al., 2006; Rogerson, Rohling, et al., 2012; Sierro et al., 1999; Stow et al., 1986; Voelker et al., 2006). The absence of a MOW impact on the sediments at this time is consistent with Mediterranean freshening related to the "African humid period" (deMenocal et al., 2000; Lézine et al., 2011; Shanahan et al., 2015) during the last Northern Hemisphere summer insolation maximum, and the relationship between enhanced runoff from northern Africa and absence of the MOW has previously been modeled by (Rogerson, Rohling, et al., 2012).

7. Impact of Surface and Intermediate Water Circulation on the Settling Depth of the MOW During HS1

During the last deglaciation, cooling of the North Atlantic during HS1 (18–14.9 kyr) was the result of southward shifts of the polar front in response to a weakened AMOC (Barker et al., 2015; Bond & Lotti, 1995; Broecker, 1994; Broecker et al., 1992; Hodell et al., 2017; Peck et al., 2006, 2007) triggered by meltwater

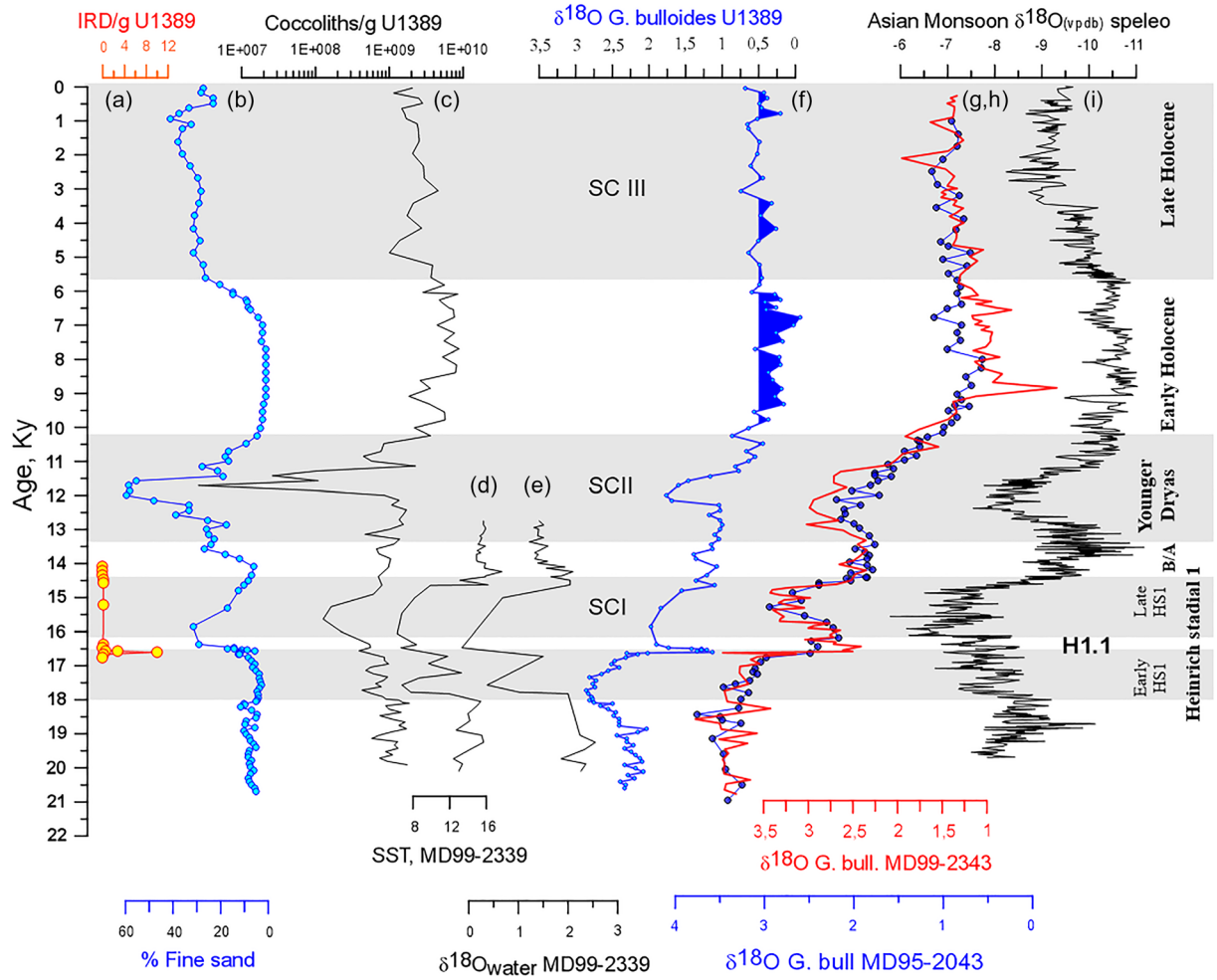

Figure 6. Changes in the velocity of the MOW at Site U1389 during the last deglaciation. Sandy contourite (SC) beds I to III were formed during the late HS1, in the YD and the late Holocene, respectively. (a) Number of IRD/g at Site U1389. (b) Percent fine sand (fraction 62–150 μm). (c) Coccoliths/g at Site U1389. (d, e) MD99-2339 SST and seawater $\delta^{18}O$ records synchronized to U1389 (Voelker et al., 2009). (f) *G. bulloides* $\delta^{18}O$ record at IODP Site U1389. (g, h) records of *G. bulloides* $\delta^{18}O$ in MD99-2343, Menorca (in red) and MD95-2043, Alboran Sea (in blue). (i) $\delta^{18}O$ from Asian speleothems (Cheng et al., 2016). G. bull denotes *G. bulloides*.

discharge during events of recession of the European and North American ice sheets (Roberts et al., 2008; Toucanne, Minto'o, et al., 2015; Toucanne, Soulet, et al., 2015; Toucanne et al., 2010; Zaragosi et al., 2001, 2006).

During HS1 two stages have been distinguished (Broecker & Putnam, 2012), the first stage (between 18 and 16.2 kyr) seems to be related to weakened AMOC triggered by meltwater derived from Eurasian and/or Laurentide ice sheets (Clark et al., 2001; Grousset et al., 2000, 2001; Hodell et al., 2017; McManus et al., 2004; Peck et al., 2007; Plaza-Morlote et al., 2017; Toucanne et al., 2010; Toucanne, Minto'o, et al., 2015) while the more extreme cooling during the second stage (16.2 to 14.7 kyr) was triggered by additional freshwater derived from large surges of icebergs originated in the Laurentide ice sheet (Broecker et al., 1992; Hodell & Curtis, 2008; Hodell et al., 2017; Plaza-Morlote et al., 2017). This second freshwater perturbation led to a more profound collapse of deep water formation in the North Atlantic and resulted in the formation of Heinrich Event 1 (H1) with deposition of IRD all over the North Atlantic. More recently a detailed study of H1 revealed that it is indeed formed by two distinct Heinrich layers deposited during the second stage of HS1, H1.1(≈16.2 kyr) and H1.2 (≈15.1 kyr) (Hodell et al., 2017). H1.1 was larger and reached the latitude of the Portuguese margin and the Strait of Gibraltar (Bard et al., 2000; de Abreu et al., 2003; Martins et al., 2013; Plaza-Morlote et al., 2017; Schonfeld et al., 2003; Zahn et al., 1997). There is a lag of around 1,500 yr between the onset of the first freshwater perturbation that triggered the onset of HS1 at around

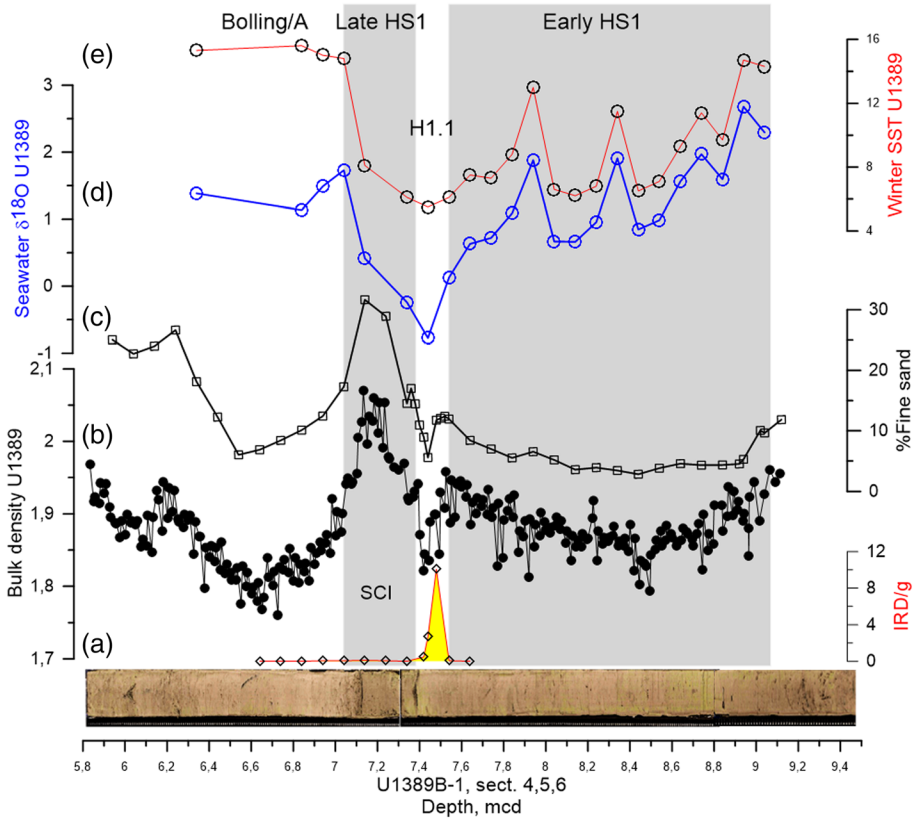

Figure 7. Changes in velocity of the MOW at Site U1389 during HS1. At the bottom, a picture of sections U1389B-1H-4, 5, and 6 is shown. The low velocity during early HS1 gradually increased toward the late HS1 with a brief notable decrease during H1.1, which is recorded by a muddy bed of around 30 cm in thickness immediately below SCI. A more detailed picture of this mud bed can be seen in Figure 8. (a) IRD per gram. (b) U1389 bulk density (Stow et al., 2013). (c) Percent fine sand (fraction 62–150 μm). (d) Seawater $\delta^{18}O$ at Site U1389, and (e) SST at Site U1389. Note that the data under 8.85 mcd shown in this figure correspond to Hole A, while the section shown in the picture is from Hole B.

18 kyr and the Laurentide iceberg surges of H1 (Barker et al., 2015; Hodell et al., 2017; Ng et al., 2018; Toucanne, Soulet, et al., 2015). The first freshwater release during the early stage of HS1 was rapidly mixed in the ocean and the freshwater anomaly was transferred to middle and deep water depths in the Atlantic, resulting in a decrease in the benthic $\delta^{18}O$ preluding the onset of H1 (Dokken & Jansen, 1999; Waelbroeck et al., 2011). However, freshening during H1, which further contributed to shut down Atlantic thermohaline circulation (McManus et al., 2004), remained at the surface for a longer time, spreading all over the Atlantic to reach the Mediterranean (Sierro et al., 2005).

To recognize the sequence of events during HS1 at Site U1389, we analyzed the SST and the number of lithic grains/g during this time period (Figures 6a, 7a, and 7e). We identified a single peak of lithic grains that we assumed were IRD during HS1. This peak was used to place Heinrich layer 1 (HL1) at Site U1389 (Figures 6a and 7a). We relate this event, which coincides with a sharp decrease of *G. bulloides* $\delta^{18}O$ and a decrease in fine sand, with H1.1 in the North Atlantic, though the age of 16.6 kyr is slightly older, but still within the age uncertainty for the radiometric dating of H1.1 at Site U1308 (Hodell et al., 2017) (Figures 6 and 7). In consequence, we relate this H1.1 with the southward expansion of the polar front (Eynaud et al., 2009) and the influence of meltwater derived from the Laurentide ice sheets at the beginning of the second stage of HS1, allowing us to place the U1389 record into the more precise internal stratigraphy of HS1 proposed by (Hodell et al., 2017).

The most likely sources for the freshwater perturbation during the early stage of HS1 are the British Scandinavian and Barents ice sheets in Europe, which drained all northwestern Europe (Dokken & Jansen, 1999; Eynaud et al., 2007; Ménot et al., 2006; Stanford et al., 2011; Toucanne et al., 2010; Zaragosi

et al., 2001, 2006) although the American ice sheets could also contribute (Clark et al., 2001). Intensive meltwater discharge to the NE Atlantic was identified in the Bay of Biscay between 18.3 and 16.7 kyr, during the early stage of HS1 (Toucanne et al., 2009, 2010; Toucanne, Soulet, et al., 2015). This freshening event was recorded by a sharp decrease of more than 3‰ in the $\delta^{18}O$ of surface waters in the Celtic margin, near the British ice sheet and was contemporaneous with a southward migration of the polar front recorded by a significant increase of the polar plantkonic foraminifer species *Neogloboquadrina pachyderma* sin (Eynaud et al., 2012). However, the largest freshening in the NE Atlantic was recorded during H1 associated to IRD coming from Laurentide ice sheet and once meltwater delivered from the Eurasian ice sheets had ceased (Eynaud et al., 2012; Zaragosi et al., 2001).

In order to see the impact of these two freshwater perturbations in the NE Atlantic we tracked them along the Iberian Margin to the Strait of Gibraltar and the Mediterranean. In the northern and central part of the Iberian margin cold and low saline waters were recorded throughout HS1 although the more negative sea-surface $\delta^{18}O$ anomalies were found during H1 (Cayre et al., 1999; Eynaud et al., 2009; Voelker et al., 2009). At Site U1389 we distinguish three episodes during HS1, similarly to what has been reported for core MD99-2339 (Voelker et al., 2006, 2009): (1) decrease of surface seawater $\delta^{18}O$ and drop of SST at around 18 kyr (Figures 7d and 7e), which correlate well with that observed in MD99-2339 (Voelker et al., 2009), and (2) arrival of warmer surface waters that preceded IRD deposition of H1.1, clearly visible in core MD99-2339 (Voelker et al., 2009) (Figures 6d and 6e) and less evident at Site U1389 (Figures 7e and 3) a second pulse of cool and very low surface seawater $\delta^{18}O$ during H1.1 (Figures 6d, 6e, 7d, and 7e).

Besides the evident similarities with core MD99-2339 (Voelker et al., 2009), this sequence of events is also seen in the SST and planktic $\delta^{18}O$ records at site MD99-2334 in offshore south Portugal and the western Mediterranean (Martrat et al., 2014; Skinner & Shackleton, 2006). We interpret this sequence of events as changes in the physicochemical properties of surface waters along the Iberian Margin and the Atlantic inflow due to the interaction between the Portugal current, which is colder and fresher, and the warmer and high saline waters of the Azores Front near the Strait of Gibraltar, confirming the scenario proposed by (Voelker et al., 2009). A higher influence of the Portugal current (lower influence of the AzC) occurred at the onset of HS1, resulting in lower seawater $\delta^{18}O$ and lower temperatures at both sides of the Strait of Gibraltar (Martrat et al., 2004, 2014; Skinner & Shackleton, 2006; Voelker et al., 2009). The warming episode at the end of the early stage of HS1 was caused by the higher influence of the AzC, typically showing higher seawater $\delta^{18}O$ and warmer SST. The imprint of this water mass in the Mediterranean is recorded by the higher $\delta^{18}O$ in *G.bulloides* and the higher SST clearly visible in the middle of HS1 (Hodell et al., 2017; Martrat et al., 2014). The influence of the AzC, however, suddenly diminished when cooler and less saline water entered the Mediterranean again during H1.1, coinciding with IRD deposition of H1.1 at Site U1389 (Figures 6a and 7a) and along the Portuguese margin and the Gulf of Cadiz (Eynaud et al., 2009; Skinner & Shackleton, 2006; Voelker et al., 2009). At Site 976 a bed with low bulk $\delta^{18}O$, which probably reflects the delivery of fine-grained carbonate by icebergs from North America, is recorded at exactly this time (Hodell et al., 2017), coinciding with a pronounced drop in salinity as reflected in the minimum $\delta^{18}O$ in the western Mediterranean planktic foraminifers (Sierro et al., 2005) (Figures 6g and 6h).

Various authors have shown that the formation of the AzC is caused by the Mediterranean overflow that sinks in the Gulf of Cadiz and generates a west-east zonal circulation cell with an eastward circulation (the AzC) that reach the Gulf of Cadiz and the Southern Iberian Margin and a westward deeper flow (the Azores countercurrent) that transport the saline MOW to the western Atlantic basin (Afanasyev et al., 2012; Carracedo et al., 2015; Comas-Rodríguez et al., 2011; Jia, 2000; Kida et al., 2008; Ozgokmen et al., 2001; Volkov & Fu, 2010). This circulation carries heat and salt to the western Iberian Margin and the Atlantic inflow through the AzC (Figure 2), which is the southernmost branch of the North Atlantic Current (NAC). This system was active during large parts of the glacial periods transporting heat to south Portugal and the Gulf of Cadiz as deduced from the high SST and the strong meridional SST gradients along the Iberian Margin (Martin-Garcia et al., 2015; Voelker & de Abreu, 2011; Voelker et al., 2009). However, during HS1, especially at the onset of HS1 and during H1.1 this system ceased to bring warm subtropical water to the Gulf of Cadiz, favoring the southward migration of the subtropical front and the advection of subpolar waters with the Portugal current to the Gulf of Cadiz and the Mediterranean.

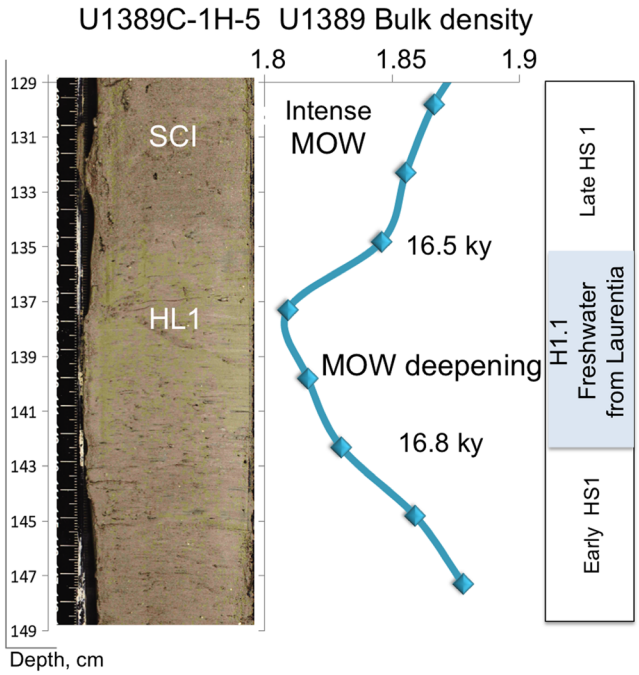

Figure 8. Picture of section U1389C-1H-5 showing the lithology of HS1 with a mud bed in the middle deposited during H1.1 and the sandy contourite SCI on top. A drop in bulk density (Stow et al., 2013) in the mud bed of H1.1 that reflects the lower strength of the MOW can be observed.

7.1. Deepening of the MOW During the Early Stage of HS1 and H1

Between 18 and 17.2 kyr, during the early stage of HS1 MOW strength at Site U1389 was lower than the average values of the last glacial maximum, and the velocity start to increase after 17 kyr parallel to the gradual weakening of Asian monsoons (Figures 6b and 7c). During the latest part of HS1, higher MOW velocities were reached at Site U1389, resulting in the formation of SCI (Figures 6b and 7). However, this gradual increase of MOW velocity was briefly interrupted by a short MOW weakening event during H1.1 (Figures 6b and 7c). These two MOW weakening events during the early stage of HS1 and H1.1 coincide with the two major freshening events in the Atlantic. In particular, the relationship between the intrusion of freshwater and weak MOW during H1.1, is clearly recorded by the decrease in grain size and bulk density (Stow et al., 2013) coinciding with a sharp drop of seawater $\delta^{18}O$ and SST at Site U1389 (Figures 6 and 7). A thin bed of more muddy sediments rich in IRD and characterized by lower bulk densities and a lower fine sand content is clearly visible (Figures 6 and 7), recording this weak MOW during H1.1. A detailed picture of this layer is shown in Figure 8.

During the second stage of HS1, the expansion of sea ice in the North Atlantic triggered by H1.1 caused extreme cool and arid conditions in the eastern Mediterranean and Red sea (Arz et al., 2003; Castaneda et al., 2010, 2016) and led to the weakest monsoon event in east Africa, India and China (Cheng et al., 2016; Shakun et al., 2007). As a result, the Mediterranean heat loss should be maximum and the Nile discharge minimum. In consequence, eastern Mediterranean heat and freshwater forcing could explain the gradual increase in MOW strength during the late stage of HS1 triggered by the higher density contrast at Gibraltar, but not the MOW weakening during H1.1 and the early stage of HS1 (Figures 7b, 7c, and 8). If this change in strength arose from altered density of outflowing Mediterranean Water, in a manner similar to velocity minima during sapropels, this would require a large freshwater discharge into the Mediterranean during H1.1. In principle, this could have come from the Fennoscandian ice sheets via the Caspian-Black Sea corridor (Bahr et al., 2005; Denton et al., 1999; Major et al., 2002, 2006; Martinez-Lamas et al., 2020; Ryan et al., 2003; Soulet et al., 2013; Tudryn et al., 2016) or from the Alps (Braakhekke et al., 2020; Monegato et al., 2017; Ravazzi et al., 2014; Tombo et al., 2015). However, within radiocarbon dating uncertainties, the timing and pattern of freshwater discharge to the Mediterranean reported by these authors does not fit with the MOW weakening events observed in this study. Consequently, we look at oceanographic changes occurring in the Atlantic as the main drivers of the MOW strength fluctuations at Site U1389. In particular we investigated the impact of Atlantic middepth circulation on the settling depth and the strength of the MOW at Site U1389, following the behavior already described in core and model data sets by Rogerson, Bigg, et al. (2012). This behavior directly links the settling depth of MOW to changes in Atlantic density gradient, and through that to AMOC strength. Near Gibraltar, a pronounced decline of North Atlantic intermediate and deep water ventilation was recorded in the Portuguese margin during HS1 using $^{231}Pa/^{230Th}$ (Gherardi et al., 2005). This reduced ventilation of Atlantic intermediate waters coincides exactly with the period of weak MOW at Site U1389. We therefore relate the two MOW weakening events observed at Site U1389 with deepenings of MOW settling depth triggered by freshwater perturbations in the North Atlantic and the resulting lower densities of middepth Atlantic water at the onset of HS1 and during H1.1. In contrast, we argue that the rising velocities starting at around 17.2 and especially after H1.1 were the result of a combination of MOW shoaling due to rising densities of middepth Atlantic waters as meltwater input decreased and cooling and drying of the eastern Mediterranean as the monsoon weakened. Similar interactions between surface and Atlantic intermediate water circulation were described in the Celtic margin (Mojtahid et al., 2017).

The MOW today spreads westward in the Atlantic below the ENACW and above the LSW and NEADW, all of them originated in the high latitudes of the north Atlancic (Figure 1) (see section 2 for references). The MOW plume flows between the northern sourced waters mentioned before and the modified AAIW that flow northward at the same depth. This scenario is the result of the competition between the Nordic overflows that sustain the high density of the intermediate and deep water, the Mediterranean overflow and the southern sourced AAIW (Bower et al., 2002; Racape et al., 2019). The relatively high density of the northern sourced waters today maintains the MOW, which is warm (>7°C) and salty, flowing over the LSW and NEADW at relatively shallow depths and block the flow of the AAIW to the north (Carracedo et al., 2016).

We interpret that the lower salinities of the Labrador, Greenland, and Norwegian seas due to the large freshwater inputs from the ice sheets, especially at the onset of HS1 and during H1.1, abruptly reduced the density of northern sourced waters, while the MOW was more dense than today (Toucanne et al., 2012) due to the negative water budget of the Mediterranean during HSs. All this forced the MOW to flow at deeper depths in the Atlantic. This decrease in density of the northern source Atlantic intermediate waters and the subsequent deepening of the MOW probably favored the northward advection of the AAIW.

The deeper flow of the MOW probably ended when the freshwater perturbations in the North Atlantic ceased and the density of the intermediate and deep water gradually recovered, pushing the MOW upward and the AAIW southward. The formation of SCI was the result of this MOW shoaling and the more extreme negative Mediterranean water budget during the last stage of HS1.

Abrupt changes of middepth circulation in the Atlantic during Heinrich events have been widely reported (Pahnke et al., 2008; Rickaby & Elderfield, 2005; Willamowski & Zahn, 2000; Yasuhara et al., 2019; Zahn & Stuber, 2002). These authors found abrupt increases in nutrient-rich waters and decrease in $\delta^{13}C$ of benthic foraminifers along the northern Moroccan margin and the western Atlantic that linked to enhanced northward advection of the southern source high nutrient AAIW at times of reduced North Atlantic overturning circulation, pointing to a competition between the glacial North Atlantic intermediate water and AAIW at intermediate water depths.

Evidence of a deeper settling of MOW in the Gulf of Cadiz during the early stage of HS1 was presented by (Rogerson et al., 2005). A large increase in fine sand content in core D13900 between 19 and 15.5 kyr records an intense MOW at around 1,300 m water depth. Similarly, Schonfeld and Zahn (2000) identified enhanced MOW activity along the Portuguese margin at 1,600–2,200 m water depth, shoaling to the current depths of 600–800 m deep near the deglaciation, probably coinciding with the gradual increase of MOW activity at Site U1389 at the end of HS1. Enhanced advection of fine-grained silty particles at 2,646 m water depth in the southern Portuguese margin was also associated to a deepening of the MOW during the first stage of HS1 (Magill et al., 2018).

During HS1 salinity must have been accumulating at intermediate depth, but shoaling of the MOW at the end of HS1 moved the flow of salt and heat upward and enhanced the northward salt transport through the NAC, preconditioning the Atlantic to return to strong overturning as suggested by (Rogerson et al., 2006). On the other hand, the injection of warm and salty water at deeper depths could have contributed to store heat in the deep North Atlantic and favored the final destabilization of the water column and abrupt overturning through the "thermobaric effect" at the base of the Bolling/Allerod as suggested by Adkins et al. (2005). The presence of warm and salty water below cold water in the deep North Atlantic during HS1 was reported by Thiagarajan et al. (2014). Although these authors assumed a Southern Ocean source for the warm and salty water in the deep North Atlantic due to its depleted radiocarbon content, a Mediterranean origin cannot be completely excluded.

8. Millennial-Scale Changes in MOW Strength and Mediterranean Overturning During MIS 3

Based on the record of fine sand, changes in MOW strength at millennial scale are evident at Site U1389. The comparison of the *G. bulloides* $\delta^{18}O$ record with the content of fine sand shows a clear link between Dansgaard-Oestcher events and variations in fine sand content (Figures 9 and 10). All D/O interstadials from GI2 to GI23 typically show very low sand contents. By contrast, Greenland stadials display high sand contents, supporting notable increases in the velocity of the MOW at Site U1389 (Figures 9c and 10).

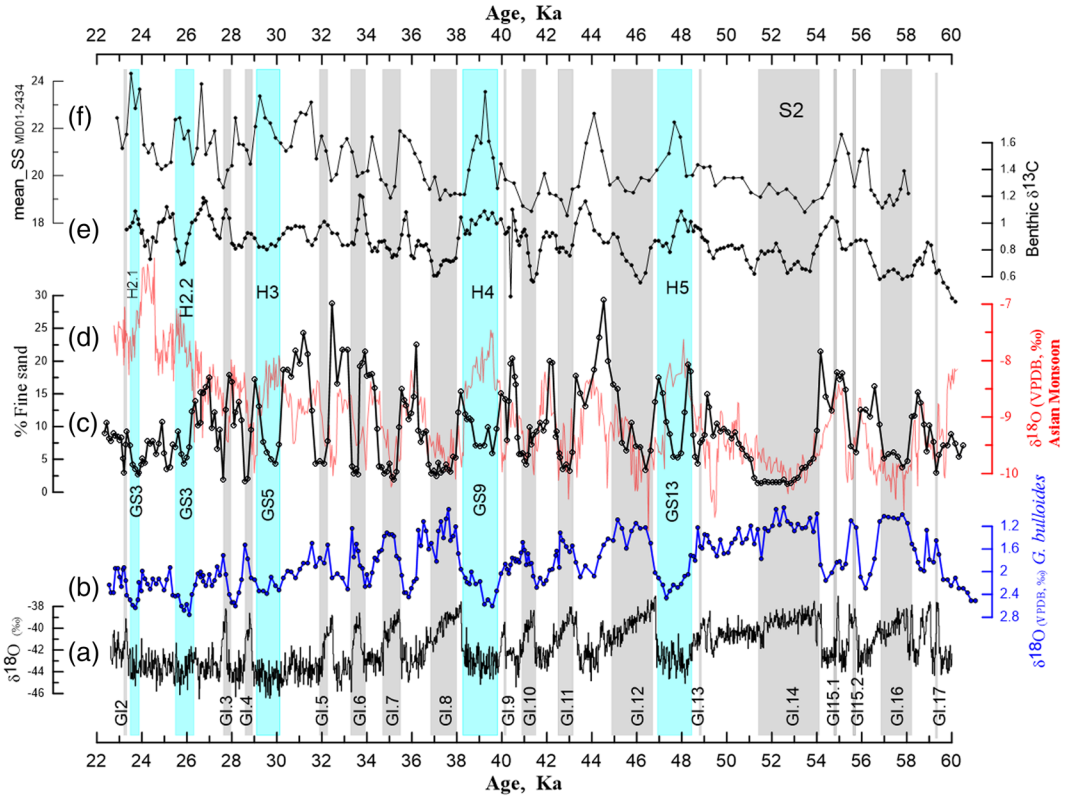

Figure 9. Millennial-scale changes in MOW strength and Mediterranean overturning at Site U1389 during MIS 3. (a) $\delta^{18}O$ NGRIP2 (‰ V-SMOW) (North Greenland Ice Core Project members, 2004) with the GICC05 timescale (Rasmussen et al., 2014). (b) *Globigerina bulloides* $\delta^{18}O$ from IODP Site U1389. (c) Percentage of fine sand (fraction 62–150 μm). (d) $\delta^{18}O$ from Asian speleothems (Cheng et al., 2016) (red). (e) *Cibicidoides pachyderma* $\delta^{13}C$ at Site U1389 (3 moving average). (f) Mean SS in the Corsica margin (MD01-2434, Toucanne et al., 2012). Gray bands show Greenland interstadials. Blue bands show HSs. GI2 to GI17 denote Greenland interstadials. GS3 to GS13 denote Greenland stadials. S2 denotes Sapropel 2.

With the exception of the HSs, the patterns of Dansgaard-Oestcher stadial-interstadial changes in MOW strength at Site U1389 are very similar to those recorded for the LIW in the Corsica margin in the western Mediterranean (Minto'o et al., 2015; Toucanne et al., 2012) (Figure 9f). This unambiguously revealed that MOW strength at Site U1389 was mainly driven by changes at Gibraltar that were, in turn, driven by variations in the rate of formation of the LIW in the eastern Mediterranean with little influence of Atlantic oceanographic conditions. The coupling between MOW strength at Site U1389 and the benthic $\delta^{13}C$ (Figure 9e) support a strong link between Mediterranean overturning circulation and the strength of the MOW at Gibraltar, with low $\delta^{13}C$ and weak overturning during Greenland interstadials and strong overturning and high $\delta^{13}C$ during stadials (Figure 9).

We interpret that these changes in MOW strength were triggered by the varying density gradients between the Mediterranean and Atlantic water at the Strait of Gibraltar, which is higher during stadials and lower during interstadials. Intense MOW typically occurs at times of cooling events in the Northern Hemisphere as was already reported by other authors (Bahr et al., 2015; Llave et al., 2006; Toucanne et al., 2007; Voelker et al., 2006). Changes in the velocity of the MOW at Gibraltar as well as in the Corsica margin must be related with Mediterranean heat and freshwater forcings, especially in the eastern Mediterranean.

A clear correspondence between high velocities of the MOW and weaker monsoon events as recorded in China speleothem records (Cheng et al., 2016; Wang et al., 2001) can be seen in Figure 9, while intense Monsoon events are unambiguously linked to weak MOW at Gibraltar, suggesting a close relationship between both events.

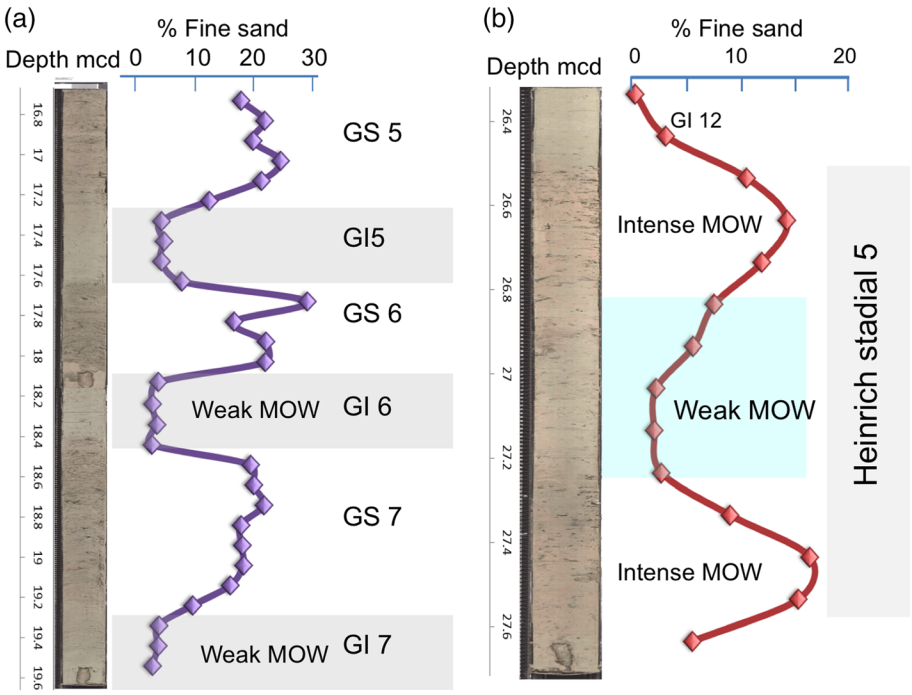

Figure 10. Pictures of Sections 3 and 4 from core U1389A-3, showing contourites during Greenland Stadials GS7, GS6, and GS5 (a) and Section 3 from core U1389A-4 (b), showing the three-stage pattern of HS5 with two contourite beds on top and bottom and a muddy interval in the middle.

During stadials, the lower rates of annual rainfall in the catchment areas of the northern Mediterranean (Sancez Goñi et al., 2002) and the expected lower Nile water discharge due to the southward shifts of the ITCZ in Africa (weaker monsoon events in Asia, Cheng et al., 2016; Wang et al., 2001), increased surface Mediterranean salinities. This more negative freshwater budget together with enhanced heat loss during winter in the areas of Mediterranean intermediate water formation triggered by a higher influence of northerly, cool winds led to higher rates of dense water formation in the Mediterranean and consequently to increase the density gradient with Atlantic water at the strait. By contrast, during interstadials, the combination of freshwater and thermal forcings increased buoyancy and substantially reduced the formation of dense, intermediate water in the western and eastern Mediterranean (Cacho et al., 2000; Sierro et al., 2005), which finally reduced the Mediterranean density gradient at Gibraltar. In consequence, parallel changes in heat and freshwater forcing seem to have governed the velocity of the MOW at Gibraltar and Mediterranean thermohaline circulation, at least at middepth, both in the eastern and western Mediterranean (Cacho et al., 2000; Frigola et al., 2008; Minto'o et al., 2015; Sierro et al., 2005; Sprovieri et al., 2012; Toucanne et al., 2012; Tripsanas et al., 2016) because both processes changed the density of Mediterranean intermediate water and therefore the density contrast at Gibraltar.

However, the strong-weak MOW activity during stadial-interstadial events described before shows notable exceptions during HSs. MOW intensity during HSs at Site U1389 is lower than in other non-HSs, in spite of being the coldest and driest periods in the Mediterranean (Figure 9). During HSs, the MOW typically shows three phases (Figures 9c and 10b), enhanced MOW at the onset and end of each HS and a weak MOW in the middle of the stadial. Each HS is characterized by silty-sandy contourite beds at the bottom and top and a finer-grained, muddy contourite bed in the middle, as shown in the picture of Figure 10b for HS5. A similar slowdown of the MOW was seen in other records from the Gulf of Cadiz (Llave et al., 2006; Toucanne et al., 2007; Voelker et al., 2006) in cores ranging from 1,170 m to 582 water depth. The strong anticorrelation between the strength of the Asian monsoons and the strength of the MOW at Site U1389 only breaks during these middle phases of HSs (Figures 9c and 9d). In addition, the parallelism between LIW velocity in the Mediterranean (Toucanne et al., 2012) and MOW strength at Site U1389 also breaks during HSs (Figure 9e). While the LIW reached maximum intensities in the Corsica margin during HSs, we

registered a weak MOW at Site U1389. Similarly, the benthic $\delta^{13}C$, which normally changes in phase with the velocity of the MOW, keeps with high values during HSs and does not register the drop in velocity seen in the middle of HSs. This suggests that the weak velocity seen in the middle of HSs is not related to Mediterranean forcing.

The drop in MOW velocity observed in the middle of each HS is clearly related to the highest planktic $\delta^{18}O$ values and the invasion of polar species to the Gulf of Cadiz, reflecting the low SST due to the southward penetration of the subpolar water. In consequence, we assume that, as already described for HS1, freshwater perturbations during HSs of the Northern Hemisphere ice sheets changed the density of middepth and deep North Atlantic waters, forcing a deepening of the more dense MOW. The characteristic three stage pattern observed in each HS at Site U1389 is the result of a delicate balance between an enhanced density of the outflow that tends to increase the velocity of the MOW in the Strait of Gibraltar and the density decrease of the Atlantic intermediate and deep water that tends to decrease the velocity of the upper core of the MOW, pushing it to higher depths. In non-HSs, the density of intermediate and deep Atlantic waters remains relatively constant and hence it is the higher density of the Ouflow what drives the increase of MOW speed at all depths. In HSs, however, the velocity of the MOW should be maximum due to the extreme Mediterranean negative water budget but its sinking to a higher water depth reduced the velocity in the shallower depths, such as at Site U1389. In fact the velocity during HSs is lower than in non-HSs. The enhanced MOW typical of all stadials, which is also visible at the onset and end of each HS, is counterbalanced by a deepening of MOW near the middle of each HS forced by the flow of the low-density northern sourced Atlantic waters.

Abrupt warming events recorded at core MD01-2444 (2,637 m deep) in the middle of HSs 4 and 5 and in other HSs can be an evidence of the influence of MOW and its associated heat flow at deeper depths along the Portuguese margin (Skinner et al., 2003; Voelker & de Abreu, 2011).

9. Impact of Orbital and Millennial Climate Changes on MOW Strength and Mediterranean Overturning During MIS 4–5 and the Origin of Sapropels S3 and S4

Changes in MOW strength during MIS 5 were the result of the interaction between orbital and millennial-scale Mediterranean climate variability. Three periods of very weak MOW during MIS 5a,c,e are linked to summer insolation maxima and the deposition of sapropels S3, S4 and S5 in the eastern Mediterranean (Figure 11) as discussed in section 5. During insolation minima, however, the velocity of the MOW increased in response to the progressively more negative water budgets in the Mediterranean, but MOW intensity was clearly punctuated by stadial-interstadial climate oscillations, following the same patterns already described for MIS 3, with more intense MOW during Greenland stadials and reduced MOW in Greenland interstadials (Figure 11). The three phase pattern of MOW velocity during HS6 and in the middle of GS22 follows the characteristic trend of HSs described in the previous section (Figure 11d).

However, MOW velocity change does not correlate with the amplitude of cooling or warming in Greenland. On the contrary, the amplitude of the millennial response of the MOW is modulated by precession, being the maximum velocities of the MOW recorded at the times of minimum NH summer insolation, regardless of the amplitude of the cooling events (Figure 11). Indeed, the coolest events in Greenland were recorded between 60 and 70 kyr during MIS 4 but MOW velocity decreased during this period, probably due to the lower summer insolation.

The high resolution record of MOW strength presented in this study allows to establish a strong connection between Greenland climate variability and sapropel formation in the eastern Mediterranean. We can conclude that the stagnation events of sappropels S3 and S4 were triggered during the abrupt warming of interstadial events GI21.1 and GI24.2, respectively (Figure 11). The sudden drop in MOW velocity seen at 84,760 and 108.280 yr can be used to accurately date the onset of sapropels S3 and S4 in the eastern Mediterranean using the Greenland chronology. They are also related to sudden northward shifts of the Asian monsoons as may be seen in Figure 11, pointing to the combination of freshwater and heat forcing at times of abrupt warming in the Northern Hemisphere as the final trigger of sapropel formation. Only the interstadial events occurring at times of precession minima caused stagnation in the estern Mediterranean. Other interestadial events such as GI19, GI20, GI22, or GI25C, even though they were of higher amplitude, never caused stagnation because they occurred during insolation minima and the average Mediterranean net freshwater

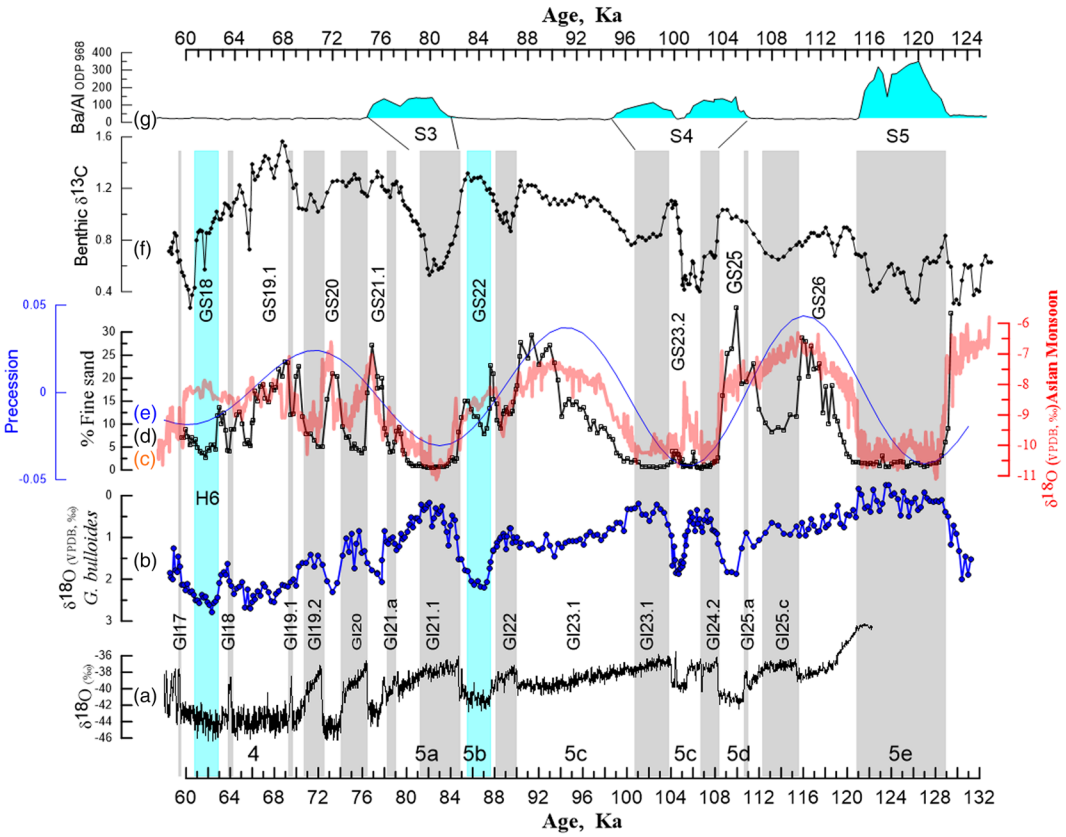

Figure 11. Millennial and orbital-scale changes in MOW strength and Mediterranean overturning during MIS 4–5. (a) $\delta^{18}O$ NGRIP2 (‰ V-SMOW) (North Greenland Ice Core Project members, 2004) with the GICC05 timescale (Rasmussen et al., 2014). (b) *Globigerina bulloides* $\delta^{18}O$ from IODP Site U1389. (c) $\delta^{18}O$ from Asian speleothems (Cheng et al., 2016) (red). (d) Percentage of fine sand (fraction 62–150 μm). (e) Precession index, (f) *Cibicidoides pachyderma* $\delta^{13}C$ at Site U1389 (3 moving average). (g) Ba/Al ratio at site ODP 968 in the eastern Mediterranean (Ziegler et al., 2008). Code numbers at the bottom denote MIS stages and substages. GI17 to GI25 and GS18 to GS26 denote Greenland interstadials and stadials, respectively. S3 to S5 denote Sapropels.

deficit was not favorable for water stratification. However, the velocity of the MOW and Mediterranean overturning substantially drop at these times as may be seen by the drecreases of fine sand and drops of benthic $\delta^{13}C$ (Figures 11d and 11f). By contrast, Greenland stadials occurring during insolation maxima, such as during S4 only caused small-amplitude increases of the MOW velocity, as it occurred during GS23.2 and GS24.1, but led to a notorius increase of Mediterranean ventilation as inferred from the high benthic $\delta^{13}C$ during GS23 that broke Mediterranean stagnation in the middle of S4.

It is important to point out that even if insolation changes are gradual and symetrical and the MOW respond to insolation, the pattern of MOW response is completely asymmetrical. The drops in MOW velocity tend to be abrupt, while the increases of MOW strength are more gradual. Indeed, MOW velocity trends follow the behavior of Dansgaard-Oestcher climate variability, characterized by abrupt warmings and more gradual coolings and, in part, the trends of Asian monsoons controlled by Northern Hemisphere climate.

The end of stagnation events in the eastern Mediterranean is recorded by a subtle increase in MOW velocity at Site U1389 and an evident increase in the benthic $\delta^{13}C$. For sapropels S3, S4 and S5, the end of stagnation approximately ocurred at glacial inceptions, as seen by the gradual increase of *G. bulloides* $\delta^{18}O$.

10. MOW During Termination II

The gradual increase of MOW strength between 150 and 138 kyr was coeval with the progressive weakening of the Asian Monsoon (Figure 12) that enhanced the rate of dense water formation in the eastern

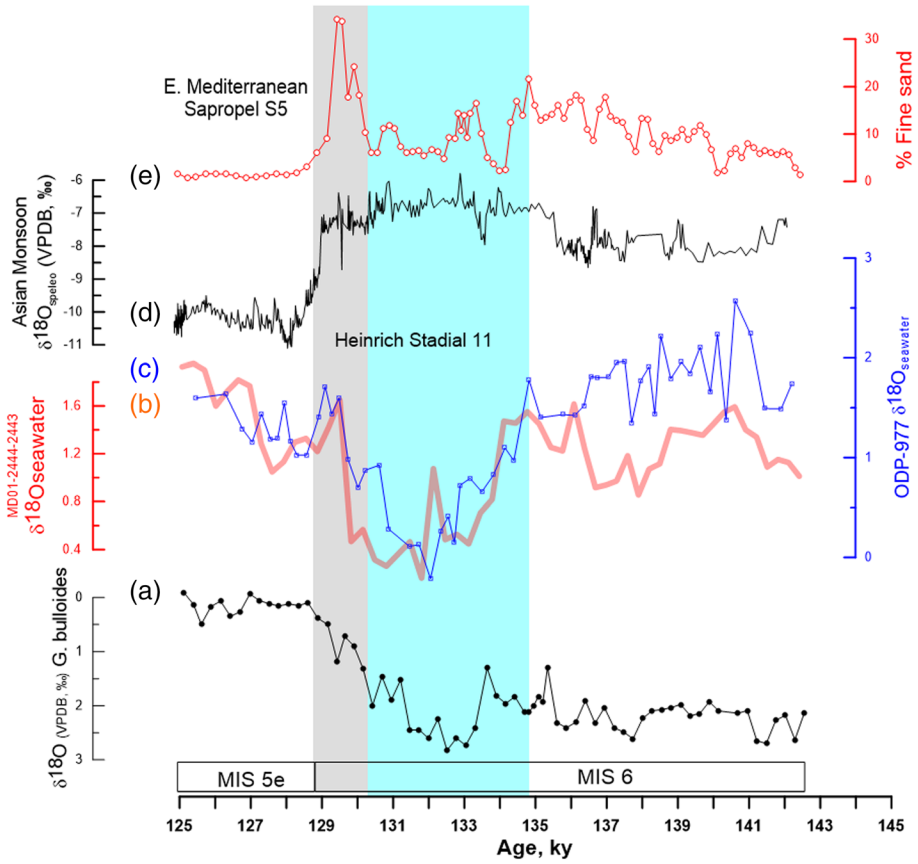

Figure 12. Relative change of MOW strength during Termination II estimated from variations in the percentage of fine sand (fraction 62–150 μm). A slower MOW is observed between 136 and 131 kyr during HS 11, coinciding with the weakest Monsoon event in Asia and a large drop of the surface water $\delta^{18}O$ in the Portuguese margin (pink) and the western Alboran basin (blue). (a) *Globigerina bulloides* $\delta^{18}O$ from IODP Site U1389. (b) Surface water $\delta^{18}O$ from core MD01-2444–2443 (it was calculated using the oxygen isotope and SST data from Hodell et al., 2013; Martrat et al., 2007), and (c) surface water $\delta^{18}O$ in ODP 977 from the western Alboran Sea (it was calculated using the isotope and SST data published by Martrat et al., 2004, and Perez-Folgado et al., 2004). Both surface water $\delta^{18}O$ records were corrected for ice volume using the sea level record of Grant et al. (2014) and a correction of 0.009‰/m. (d) $\delta^{18}O_{speleothem}$ from Cheng et al. (2016). (e) Percent fine sand (fraction 62–150 μm). Gray and blue bands mark the weak and strong MOW phases during HS11.

Mediterranean and the higher density contrast at Gibraltar. This trend toward higher surface water densities in the eastern Mediterranean should have reached maximum values during the pronounced weak Asian monsoon event of HS11 (Cheng et al., 2006, 2016; Kelly et al., 2006) (Figure 12) triggered by the collapse of the AMOC in the Atlantic (Oppo et al., 2006). However, during the early stage of HS11 the MOW velocity decreases at Site U1389 as recorded by the lower fine sand percentages between 136 and 132 kyr (Figure 12), similarly to what has been described for HS1. This weaker MOW at Site U1389 coincided with a significant freshwater anomaly that reached the Southern Portuguese margin and entered the Mediterranean sea as can be seen in the surface water $\delta^{18}O$ drop at sites MD01-2444 (sea water $\delta^{18}O$ calculated from $\delta^{18}O$ and SST data published by Hodell et al. (2013) and Martrat et al. (2007) and ODP 977 in the Alboran Sea (seawater $\delta^{18}O$ calculated using $\delta^{18}O$ data and SST published by Perez-Folgado et al. (2004) (Figure 12). This freshwater anomaly was accompanied by IRD deposition along the Portuguese margin (Skinner & Shackleton, 2006) and a similar freshwater perturbation in the deep-water $\delta^{18}O$. This Atlantic freshwater intrusion was also detected in the western Mediterranean (Jimenez-Amat & Zahn, 2015; Marino et al., 2015; Martrat et al., 2014; Perez-Folgado et al., 2004) and eastern Mediterranean (Grant et al., 2016).

As for HS1, we conclude that these low MOW velocities at the depth of Site U1389 were the result of a MOW deepening triggered by a decrease in density of the Atlantic intermediate and deep waters to the west of the Camarinal sill. This scenario started to change at the end of HS11 when the gradual recovery of the density of intermediate and deep water in the NE Atlantic forced the MOW to shoal, reaching again the depth of Site U1389. This shoaling of the MOW probably increased the injection of salt and heat at shallower depths in the Atlantic 2 kyr earlier than the reinitiation of overturning in the Atlantic. The long duration of HS11 could have favored a larger accumulation of heat and salt in the intermediate Atlantic leading to a more rapid deglaciation during Termination II (Clark et al., 2020).

11. Conclusions

The analysis of sediment cores at IODP Site U1389 revealed the presence of sandy silty contourite beds interbedded in more muddy intervals. An increase in strength of the MOW at Site U1389 washed the bottom sediments, winnowing the fine-grained particles and concentrating the coarse ones, resulting in the formation of sandy silty contourite beds. In contrast, a weakening of the MOW led to more hemipelagic sedimentation characterized by a higher accumulation of pelagic-rich calcareous sediments. Over the last 250 kyr, 10 muddy, more hemipelagic intervals record pronounced drops of MOW strength at Gibraltar at times of Northern Hemisphere summer insolation maxima and were correlated with the deposition of sapropels S1 to S9 in the eastern Mediterranean. Besides the low MOW velocity, the pronounced drops of the benthic $\delta^{13}C$ record the weak Mediterranean overturning circulation at times of sapropel deposition. The higher annual rainfall in perimediterranean areas and the northward shift of the ITCZ in equatorial Africa increased the freshwater discharge to the Mediterranean and decreased the dense water formation in the Levantine seas and the density gradient between the Atlantic and Mediterranean water at Gibraltar. In contrast, between these more hemipelagic intervals, sandy silty contourite beds were formed due to the higher velocities of the MOW at Gibraltar. They were associated to strong Mediterranean overturning circulation as reflected by the high benthic $\delta^{13}C$. The formation of these sandy silty contourites were the result of higher density gradients between the outflow and inflow at Gibraltar due to the more negative water budgets in the Mediterranean at summer insolation minima when African monsoons were weak.

Millennial-scale oscillations in Mediterranean net freshwater loss with likely additional effects from heat forcing on the northern margin were also responsible for the changes in MOW strength during MIS 3 and MIS 5. The stagnation events of sappropels S3 and S4 were triggered during the abrupt warming of interstadial events GI21.1 and GI24.2, respectively. These events are recorded in the Gulf of Cadiz by a sudden drop in MOW velocity and a decrease of benthic $\delta^{13}C$ at 84,760 and 108,280 yr, based on the Greenland chronology.

The higher net freshwater loss during Greenland stadials, which was also linked to weak African monsoons, triggered higher speeds of the MOW at Gibraltar due to the higher density contrast between the outflow and inflow. However, a notable exception to this pattern was recognized during HSs. Although they are characterized by the weakest African monsoons and the more extreme net freshwater losses in the Mediterranean, the MOW speed at Site U1389 declined, especially in the middle of the HSs. We concluded that these drops of the MOW velocity in the middle of HSs at Site U1389 were not triggered by MOW strength weakenings but with deepenings of the MOW settling depth in the Atlantic. These deepenings were especially notable during HS1 and HS11 at Terminations I and II and were always associated to significant drops of sea surface $\delta^{18}O$ in the Gulf of Cadiz and western Mediterranean. The events of freshwater discharge from the Eurasian and North American ice sheets during HSs reduced sea surface salinity in the Labrador, Greenland, and Norwegian seas and thus the density of the intermediate and deep waters of the North Atlantic. This reduced the vertical density gradient to the west of Gibraltar, resulting in a deepening of the higher density MOW. The intrusion of salt and heat at deeper depths in the NE Atlantic at times of injection of low-salinity waters in the northern latitudes probably modified the meridional density gradient with consequences for the AMOC. The shoaling of the MOW and thus the shallower injection of salt and heat observed at the end of HS1 and HS11 could have favored the reinitiation of the Atlantic overturning, especially at the end of HS1 and HS11.

Data Availability Statement

The data are available in the Pangaea online database (https://doi.pangaea.de/10.1594/PANGAEA.921470).

Acknowledgments

This work was funded by the Ministry of Economy of Spain Project RTI2018-099489-B-I00, CGL2015-68459-P, and Junta de Castilla y León (UIC 102). We appreciate the work of Jose Ignacio Martin Cruz in sample processing and the picking of planktic and benthic foraminifers. We are very grateful to IODP for inviting some of us to participate in Expedition 339 Mediterranean Outflow and providing the samples used in this study. Part of this work has been done in colaboration with "The Drifters" Research Group at Royal Holloway University of London (RHUL), and it is related to the projects CTM 2012-39599-C03, CGL2016-80445-R, and CTM2016-75129-C3-1-R. Also, we thank *María Druet* (IGME, Spain) for their help in the base map for Figure 1c. Suggestions and comments from Dr. Antje Voelker and Samuel Toucanne were very helpful and substantially improved the last version of this manuscript.

References

Adkins, J. F., Ingersoll, A. P., & Pasquero, C. (2005). Rapid climate change and conditional instability of the glacial deep ocean from the thermobaric effect and geothermal heating. *Quaternary Science Reviews*, *24*(5-6), 581–594. https://doi.org/10.1016/j.quascirev.2004.11.005

Afanasyev, Y. D., O'Leary, S., Rhines, P. B., & Lindahl, E. (2012). On the origin of jets in the ocean. *Geophysical and Astrophysical Fluid Dynamics*, *106*(2), 113–137. doi.org/10.1080/03091929.2011.562896

Ambar, I., & Howe, M. R. (1979). Observations of the Mediterranean Outflow—I Mixing in the Mediterranean Outflow. *Deep Sea Research Part A, Oceanographic Research Papers*, *26*(5), 535–554. https://doi.org/10.1016/0198-0149(79)90095-5

Arz, H. W., Patzold, J., Muller, P. J., & Moammar, M. O. (2003). Influence of Northern Hemisphere climate and global sea level rise on the restricted Red Sea marine environment during termination I. *Paleoceanography*, *18*, 1053. https://doi.org/10.1029/2002pa000864

Bahr, A., Kaboth, S., Jiménez-Espejo, F. J., Sierro, F. J., Voelker, A. H. L., Lourens, L., et al. (2015). Persistent monsoonal forcing of Mediterranean Outflow water dynamics during the late Pleistocene. *Geology*, *43*(11), 951–954. https://doi.org/10.1130/G37013.1

Bahr, A., Lamy, F., Arz, H., Kuhlmann, H., & Wefer, G. (2005). Late glacial to Holocene climate and sedimentation history in the NW Black Sea. *Marine Geology*, *214*(4), 309–322. https://doi.org/10.1016/j.margeo.2004.11.013

Bard, E., Rostek, F., Turon, J. L., & Gendreau, S. (2000). Hydrological impact of Heinrich events in the subtropical northeast Atlantic. *Science*, *289*(5483), 1321–1324. https://doi.org/10.1126/science.289.5483.1321

Baringer, M. O., & Price, J. F. (1997). Mixing and spreading of the Mediterranean Outflow. *Journal of Physical Oceanography, 27*(8), 1654-1677. https://doi:10.1175/1520-0485(1997)027<1654:masotm>2.0.co;2

Barker, S., Chen, J., Gong, X., Jonkers, L., Knorr, G., & Thornalley, D. (2015). Icebergs not the trigger for North Atlantic cold events. *Nature*, *520*(7547), 333–336. https://doi.org/10.1038/nature14330

Barker, S., Knorr, G., Edwards, R. L., Parrenin, F., Putnam, A. E., Skinner, L. C., et al. (2011). 800,000 years of abrupt climate variability. *Science*, *334*(6054), 347–351. https://doi.org/10.1126/science.1203580

Bar-Matthews, M., Ayalon, A., & Kaufman, A. (2000). Timing and hydrological conditions of Sapropel events in the eastern Mediterranean, as evident from speleothems, Soreq cave, Israel. *Chemical Geology*, *169*(1-2), 145–156. https://doi.org/10.1016/s0009-2541(99)00232-6

Bashmachnikov, I., Nascimento, A., Neves, F., Menezes, T., & Koldunov, N. V. (2015). Distribution of intermediate water masses in the subtropical northeast Atlantic. *Ocean Science*, *11*(5), 803–827. https://doi.org/10.5194/os-11-803-2015

Bethoux, J. P. (1979). Budgets of the Mediterranean Sea. Their dependance on the local climate and on the characteristics of the Atlantic waters. *Oceanologica Acta*, *2*(2), 157–163. doi.org/10.1007/s00367-006-0048-9

Bethoux, J. P., & Gentili, B. (1999). Functioning of the Mediterranean Sea: Past and present changes related to freshwater input and climate changes. *Journal of Marine Systems*, *20*(1-4), 33–47. https://doi.org/10.1016/s0924-7963(98)00069-4

Bethoux, J. P., Gentili, B., Morin, P., Nicolas, E., Pierre, C., & Ruiz-Pino, D. (1999). The Mediterranean Sea: A miniature ocean for climatic and environmental studies and a key for the climatic functioning of the North Atlantic. *Progress in Oceanography*, *44*(1-3), 131–146. https://doi.org/10.1016/s0079-6611(99)00023-3

Bethoux, J. P., & Pierre, C. (1999). Mediterranean functioning and sapropel formation: Respective influences of climate and hydrological changes in the Atlantic and the Mediterranean. *Marine Geology*, *153*(1-4), 29–39. https://doi.org/10.1016/s0025-3227(98)00091-7

Bond, G. C., & Lotti, R. (1995). Iceberg discharges into the North Atlantic on millennial time scales during the last glaciation. *Science*, *267*(5200), 1005–1010. https://doi.org/10.1126/science.267.5200.1005

Bosmans, J. H. C., Drijfhout, S. S., Tuenter, E., Hilgen, F. J., & Lourens, L. J. (2015). Response of the North African summer monsoon to precession and obliquity forcings in the EC-Earth GCM. *Climate Dynamics*, *44*(1-2), 279–297. https://doi.org/10.1007/s00382-014-2260-z

Bosmans, J. H. C., van der Ent, R. J., Haarsma, R. J., Drijfhout, S. S., & Hilgen, F. J. (2020). Precession-and obliquity-induced changes in moisture sources for enhanced precipitation over the Mediterranean Sea. *Paleoceanography and Paleoclimatology*, *35*(1), e2019PA003655. https://doi.org/10.1029/2019PA003655

Boswell, S. M., Toucanne, S., Pitel-Roudaut, M., Creyts, T. T., Eynaud, F., & Bayon, G. (2019). Enhanced surface melting of the Fennoscandian Ice Sheet during periods of North Atlantic cooling. *Geology*, *47*(7), 664–668.

Bower, A. S., Le Cann, B., Rossby, T., Zenk, W., Gould, J., Speer, K., et al. (2002). Directly measured mid-depth circulation in the northeastern North Atlantic Ocean. *Nature*, *419*(6907), 603–607. https://doi.org/10.1038/nature01078

Boyer, T. P., Baranova, O. K., Coleman, C., Garcia, H. E., Grodsky, A., Locarnini, R. A., et al. (2018). World Ocean Database. In A. V. Mishonov (Ed.), *NOAA Atlas NESDIS 87*.

Braakhekke, J., Ivy-Ochs, S., Monegato, G., Gianotti, F., Martin, S., Casale, S., & Christl, M. (2020). Timing and flow pattern of the Orta Glacier (European Alps) during the Last Glacial Maximum. *Boreas*, *18*. https://doi.org/10.1111/bor.12427

Brackenridge, R. E., Stow, D. A., Hernández-Molina, F. J., Jones, C., Mena, A., Alejo, I., et al. (2018). Textural characteristics and facies of sand-rich contourite depositional systems. *Sedimentology*, *65*(7), 2223–2252. https://doi.org/10.1111/sed.12463

Broecker, W., Bond, G., Klas, M., Clark, E., & McManus, J. (1992). Origin of the northern Atlantic's Heinrich events. *Climate Dynamics*, *6*(3-4), 265–273. http://doi.org/10.1007/BF00193540

Broecker, W., & Putnam, A. E. (2012). How did the hydrologic cycle respond to the two-phase mystery interval? *Quaternary Science Reviews*, *57*, 17–25. https://doi.org/10.1016/j.quascirev.2012.09.024

Broecker, W. S. (1994). Massive iceberg discharges as triggers for global climate change. *Nature*, *372*(6505), 421–424. https://doi.org/10.1038/372421a0

Bryden, H. L., Candela, J., & Kinder, T. H. (1994). Exchange through the Strait of Gibraltar. *Progress in Oceanography*, *33*(3), 201–248. https://doi.org/10.1016/0079-6611(94)90028-0

Bryden, H. L., & Kinder, T. H. (1991). Steady 2-layer exchange through the Strait of Gibraltar. *Deep-Sea Research Part A-Oceanographic Research Papers, 38,* S445-S463. doi.org/10.1016/S0198-0149(12)80020-3

Bryden, H. L., & Stommel, H. M. (1982). Origin of the Mediterranean Outflow. *Journal of Marine Research*, *40*, 55–71.

Bryden, H. L., & Stommel, H. M. (1984). Limiting processes that determine basic features of the circulation in the Mediterranean-Sea. *Oceanologica Acta*, *7*(3), 289–296.

Cacho, I., Grimalt, J. O., Sierro, F. J., Shackleton, N., & Canals, M. (2000). Evidence for enhanced Mediterranean thermohaline circulation during rapid climatic coolings. *Earth and Planetary Science Letters*, *183*(3-4), 417–429. https://doi.org/10.1016/S0012-821X(00)00296-X

Carracedo, L. I., Gilcoto, M., Mercier, H., & Perez, F. F. (2015). Quasi-synoptic transport, budgets and water mass transformation in the Azores-Gibraltar Strait region during summer 2009. *Progress in Oceanography*, *130*, 47–64. https://doi.org/10.1016/j.pocean.2014.09.006

Carracedo, L. I., Pardo, P. C., Flecha, S., & Perez, F. F. (2016). On the Mediterranean water composition. *Journal of Physical Oceanography*, *46*(4), 1339–1358. https://doi.org/10.1175/jpo-d-15-0095.1

Castaneda, I. S., Schefuss, E., Patzold, J., Damste, J. S. S., Weldeab, S., & Schouten, S. (2010). Millennial-scale sea surface temperature changes in the eastern Mediterranean (Nile River Delta region) over the last 27,000 years. *Paleoceanography*, *25*. https://doi.org/10.1029/2009pa001740

Castañeda, I. S., Schouten, S., Pätzold, J., Lucassen, F., Kasemann, S., Kuhlmann, H., & Schefuß, E. (2016). Hydroclimate variability in the Nile River Basin during the past 28,000 years. *Earth and Planetary Science Letters*, *438*, 47–56. https://doi.org/10.1016/j.epsl.2015.12.014

Cayre, O., Lancelot, Y., & Vincent, E. (1999). Paleoceanographic reconstructions from planktonic foraminifera off the Iberian Margin: Temperature, salinity, and Heinrich events. *Paleoceanography*, *14*(3), 384–396. https://doi.org/10.1029/1998pa900027

Cheng, H., Edwards, R. L., Sinha, A., Spötl, C., Yi, L., Chen, S., et al. (2016). The Asian monsoon over the past 640,000 years and ice age terminations. *Nature*, *534*(7609), 640. https://doi.org/10.1038/nature18591

Cheng, H., Edwards, R. L., Wang, Y., Kong, X., Ming, Y., Kelly, M. J., et al. (2006). A penultimate glacial monsoon record from Hulu Cave and two-phase glacial terminations. *Geology*, *34*(3), 217–220. https://doi.org/10.1130/g22289.1

Clark, P. U., He, F., Golledge, N. R., Mitrovica, J. X., Dutton, A., Hoffman, J. S., & Dendy, S. (2020). Oceanic forcing of penultimate deglacial and last interglacial sea-level rise. *Nature*, *577*, 660–664. https://doi.org/10.1038/s41586-020-1931-7

Clark, P. U., Marshall, S. J., Clarke, G. K. C., Hostetler, S. W., Licciardi, J. M., & Teller, J. T. (2001). Freshwater forcing of abrupt climate change during the last glaciation. *Science*, *293*(5528), 283–287. https://doi.org/10.1126/science.1062517

Comas-Rodríguez, I., Hernández-Guerra, A., Fraile-Nuez, E., Martínez-Marrero, A., Benítez-Barrios, V. M., Pérez-Hernández, M. D., & Vélez-Belchí, P. (2011). The Azores Current System from a meridional section at 24.5°W. *Journal of Geophysical Research*, *116*, 9. https://doi.org/10.1029/2011jc007129

Cornuault, M., Vidal, L., Tachikawa, K., Licari, L., Rouaud, G., Sonzogni, C., & Revel, M. (2016). Deep water circulation within the eastern Mediterranean Sea over the last 95 kyr: New insights from stable isotopes and benthic foraminiferal assemblages. *Palaeogeography, Palaeoclimatology, Palaeoecology*, *459*, 1–14. https://doi.org/10.1016/j.palaeo.2016.06.038

Criado-Aldeanueva, F., Javier Soto-Navarro, F., & Garcia-Lafuente, J. (2012). Seasonal and interannual variability of surface heat and freshwater fluxes in the Mediterranean Sea: Budgets and exchange through the Strait of Gibraltar. *International Journal of Climatology*, *32*(2), 286–302. https://doi.org/10.1002/joc.2268

de Abreu, L., Shackleton, N. J., Schonfeld, J., Hall, M., & Chapman, M. (2003). Millennial-scale oceanic climate variability off the western Iberian Margin during the last two glacial periods. *Marine Geology*, *196*(1-2), 1–20. https://doi.org/10.1016/s0025-3227(03)00046-x

de Castro, S., Hernández-Molina, F. J., Rodríguez-Tovar, F. J., Llave, E., Ng, Z. L., Nishida, N., & Mena, A. (2020). Contourites and bottom current reworked sands: Bed facies model and implications. *Marine Geology*, 428. https://doi.org/10.1016/j.margeo.2020.106267

deMenocal, P., Ortiz, J., Guilderson, T., Adkins, J., Sarnthein, M., Baker, L., & Yarusinsky, M. (2000). Abrupt onset and termination of the African humid period: Rapid climate responses to gradual insolation forcing. *Quaternary Science Reviews*, *19*(1–5), 347–361. https://doi.org/10.1016/S0277-3791(99)00081-5

Denton, G. H., Heusser, C. J., Lowel, T. V., Moreno, P. I., Andersen, B. G., Heusser, L. E., et al. (1999). Interhemispheric linkage of paleoclimate during the last glaciation. *Geografiska Annaler Series A-Physical Geography*, *81A*(2), 107–153. https://doi.org/10.1111/j.0435-3676.1999.00055.x

Dokken, T. M., & Jansen, E. (1999). Rapid changes in the mechanism of ocean convection during the last glacial period. *Nature*, *401*(6752), 458–461. https://doi.org/10.1038/46753

Eynaud, F., De Abreu, L., Voelker, A., Schönfeld, J., Salgueiro, E., Turon, J. L., et al. (2009). Position of the Polar Front along the western Iberian Margin during key cold episodes of the last 45 ka. *Geochemistry Geophysics Geosystems*, *10*. https://doi.org/10.1029/2009gc002398

Eynaud, F., Malaizé, B., Zaragosi, S., de Vernal, A., Scourse, J., Pujol, C., et al. (2012). New constraints on European glacial freshwater releases to the North Atlantic Ocean. *Geophysical Research Letters*, *39*(15), L15601. https://doi.org/10.1029/2012gl052100

Eynaud, F., Zaragosi, S., Scourse, J. D., Mojtahid, M., Bourillet, J. F., Hall, I. R., et al. (2007). Deglacial laminated facies on the NW European continental margin: The hydrographic significance of British-Irish Ice Sheet deglaciation and Fleuve Manche paleoriver discharges. *Geochemistry Geophysics Geosystems*, 8. https://doi.org/10.1029/2006gc001496

Faugeres, J. C., Gonthier, E., & Stow, D. A. V. (1984). Contourite drift molded by deep Mediterranean Outflow. *Geology, 12*(5), 296-300. https://doi.org/10.1130/0091-7613(1984)12<296:cdmbdm>2.0.co;2

Fichaut, M., Garcia, M. J., Giorgetti, A., Iona, A., Kuznetsov, A., Rixen, M., & Group, M (2003). MEDAR/MEDATLAS 2002: A Mediterranean and Black Sea database for operational oceanography. In H. Dahlin, N. C. Flemming, S. E. Petersson, & K. Nittis (Eds.), *Building the European capacity in operational oceanography, proceedings* (Vol. 69, pp. 645–648). Amsterdam: Elsevier Science Bv.

Flores, J. A., & Sierro, F. J. (1997). Revised technique for calculation of calcareous nannofossil accumulation rates. *Micropaleontology*, *43*(3), 321–324. https://doi.org/10.2307/1485832

Frigola, J., Moreno, A., Cacho, I., Canals, M., Sierro, F. J., Flores, J. A. & Grimalt, J. O. (2008). Evidence of abrupt changes in western Mediterranean deep water circulation during the last 50 kyr: A high-resolution marine record from the Balearic Sea. *Quaternary International, 181,* 88-104. doi.org/10.1016/S0012-821X(00)00296-X

Garcia-Lafuente, J., Naranjo, C., Sammartino, S., Sanchez-Garrido, J. C., & Delgado, J. (2017). The Mediterranean Outflow in the Strait of Gibraltar and its connection with upstream conditions in the Alboran Sea. *Ocean Science*, *13*(2), 195–207. https://doi.org/10.5194/os-13-195-2017

Gasser, M., Pelegrí, J. L., Emelianov, M., Bruno, M., Gràcia, E., Pastor, M., et al. (2017). Tracking the Mediterranean Outflow in the Gulf of Cadiz. *Progress in Oceanography*, *157*, 47–71. https://doi.org/10.1016/j.pocean.2017.05.015

Gherardi, J. M., Labeyrie, L., McManus, J. F., Francois, R., Skinner, L. C., & Cortijo, E. (2005). Evidence from the Northeastern Atlantic basin for variability in the rate of the meridional overturning circulation through the last deglaciation. *Earth and Planetary Science Letters*, *240*(3-4), 710–723. https://doi.org/10.1016/j.epsl.2005.09.061

Gonthier, E. G., Faugères, J. C., & Stow, D. A. V. (1984). Contourite facies of the Faro drift, Gulf of Cadiz. *Geological Society, London, Special Publications*, *15*(1), 275–292. https://doi.org/10.1144/GSL.SP.1984.015.01.18

Grant, K. M., Grimm, R., Mikolajewicz, U., Marino, G., Ziegler, M., & Rohling, E. J. (2016). The timing of Mediterranean sapropel deposition relative to insolation, sea-level and African monsoon changes. *Quaternary Science Reviews*, *140*, 125–141. https://doi.org/10.1016/j.quascirev.2016.03.026

Grant, K. M., Rohling, E. J., Ramsey, C. B., Cheng, H., Edwards, R. L., Florindo, F., et al. (2014). Sea-level variability over five glacial cycles. *Nature Communications*, *5*(1), 1–9.

Grousset, F. E., Cortijo, E., Huon, S., Hervé, L., Richter, T., Burdloff, D., et al. (2001). Zooming in on Heinrich layers. *Paleoceanography*, *16*(3), 240–259. https://doi.org/10.1029/2000pa000559

Grousset, F. E., Pujol, C., Labeyrie, L., Auffret, G., & Boelaert, A. (2000). Were the North Atlantic Heinrich events triggered by the behavior of the European ice sheets? *Geology*, *28*(2), 123–126.

Hernández-Molina, F. J., Llave, E., Preu, B., Ercilla, G., Fontan, A., Bruno, M., et al. (2014). Contourite processes associated with the Mediterranean Outflow water after its exit from the Strait of Gibraltar: Global and conceptual implications. *Geology*, *42*(3), 227–230. https://doi.org/10.1130/g35083.1

Hernández-Molina, F. J., Sierro, F. J., Llave, E., Roque, C., Stow, D. A. V., Williams, T., et al. (2016). Evolution of the gulf of Cadiz margin and southwest Portugal contourite depositional system: Tectonic, sedimentary and paleoceanographic implications from IODP expedition 339. *Marine Geology*, *377*, 7–39. https://doi.org/10.1016/j.margeo.2015.09.013

Hernández-Molina, J., Llave, E., Somoza, L., Fernández-Puga, M.C., Maestro, A., León, R., et al. (2003). Looking for clues to paleoceanographic imprints: A diagnosis of the Gulf of Cadiz contourite depositional systems. *Geology, 31*(1), 19-22. https://doi.org/10.1130/0091-7613(2003)031<0019:lfctpi>2.0.co;2

Hodell, D., Crowhurst, S., Skinner, L., Tzedakis, P. C., Margari, V., Channell, J. E., et al. (2013). Response of Iberian Margin sediments to orbital and suborbital forcing over the past 420 ka. *Paleoceanography*, *28*, 185–199.

Hodell, D. A., & Curtis, J. H. (2008). Oxygen and carbon isotopes of detrital carbonate in North Atlantic Heinrich events. *Marine Geology*, *256*(1-4), 30–35. https://doi.org/10.1016/j.margeo.2008.09.010

Hodell, D. A., Nicholl, J. A., Bontognali, T. R., Danino, S., Dorador, J., Dowdeswell, J. A., et al. (2017). Anatomy of Heinrich Layer 1 and its role in the last deglaciation. *Paleoceanography*, *32*, 284–303. http://doi.org/10.1002/2016PA003028

Hoffmann, D. L., Rogerson, M., Spötl, C., Luetscher, M., Vance, D., Osborne, A. H., et al. (2016). Timing and causes of North African wet phases during the last glacial period and implications for modern human migration. *Scientific Reports*, *6*, 7. https://doi.org/10.1038/srep36367

Iorga, M. C., & Lozier, M. S. (1999). Signatures of the Mediterranean Outflow from a North Atlantic climatology 1. Salinity and density fields. *Journal of Geophysical Research*, *104*(C11), 25, 985–26, 009. http://doi.org/10.1029/1999JC900115

Ivanovic, R. F., Valdes, P. J., Gregoire, L., Flecker, R., & Gutjahr, M. (2014). Sensitivity of modern climate to the presence, strength and salinity of Mediterranean-Atlantic exchange in a global general circulation model. *Climate Dynamics*, *42*(3-4), 859–877. https://doi.org/10.1007/s00382-013-1680-5

Jia, Y. L. (2000). Formation of an Azores Current due to Mediterranean overflow in a modeling study of the North Atlantic. *Journal of Physical Oceanography*, *30*(9), 2342-2358. https://doi.org/10.1175/1520-0485(2000)030<2342:FOAACD>2.0.CO;2

Jimenez-Amat, P., & Zahn, R. (2015). Offset timing of climate oscillations during the last two glacial-interglacial transitions connected with large-scale freshwater perturbation. *Paleoceanography*, *30*, 768–788. https://doi.org/10.1002/2014pa002710

Jorda, G., Sanchez-Roman, A., & Gomis, D. (2017). Reconstruction of transports through the Strait of Gibraltar from limited observations. *Climate Dynamics*, *48*(3-4), 851–865. https://doi.org/10.1007/s00382-016-3113-8

Jorda, G., Von Schuckmann, K., Josey, S. A., Caniaux, G., García-Lafuente, J., Sammartino, S., et al. (2017). The Mediterranean Sea heat and mass budgets: Estimates, uncertainties and perspectives. *Progress in Oceanography*, *156*, 174–208. https://doi.org/10.1016/j.pocean.2017.07.001

Josey, S. A. (2003). Changes in the heat and freshwater forcing of the eastern Mediterranean and their influence on deep water formation. *Journal of Geophysical Research*, *108*(C7). https://doi.org/10.1029/2003jc001778

Kaboth, S., Bahr, A., Reichart, G. J., Jacobs, B., & Lourens, L. J. (2016). New insights into upper MOW variability over the last 150 kyr from IODP 339 Site U1386 in the Gulf of Cadiz. *Marine Geology*, *377*, 136–145. https://doi.org/10.1016/j.margeo.2015.08.014

Kaboth, S., de Boer, B., Bahr, A., Zeeden, C., & Lourens, L. J. (2017). Mediterranean Outflow water dynamics during the past similar to 570 kyr: Regional and global implications. *Paleoceanography*, *32*(6), 634–647. https://doi.org/10.1002/2016pa003063

Kaboth, S., Grunert, P., & Lourens, L. (2017). Mediterranean Outflow water variability during the Early Pleistocene. *Climate of the Past*, *13*, 1023–1035. https://doi.org/10.5194/cp-13-1023-2017

Kaboth-Bahr, S., Bahr, A., Zeeden, C., Toucanne, S., Eynaud, F., Jiménez-Espejo, F., et al. (2018). Monsoonal forcing of European ice-sheet dynamics during the Late Quaternary. *Geophysical Research Letters*, *45*, 7066–7074. https://doi.org/10.1029/2018gl078751

Kelly, M. J., Edwards, R. L., Cheng, H., Yuan, D., Cai, Y., Zhang, M., et al. (2006). High resolution characterization of the Asian Monsoon between 146,000 and 99,000 years BP from Dongge Cave, China and global correlation of events surrounding Termination II. *Palaeogeography Palaeoclimatology Palaeoecology*, *236*(1-2), 20–38. https://doi.org/10.1016/j.palaeo.2005.11.042

Kida, S., Price, J. F., & Yang, J. (2008). The upper-oceanic response to overflows: A mechanism for the Azores Current. *Journal of Physical Oceanography*, *38*(4), 880–895. https://doi.org/10.1175/2007jpo3750.1

Kubin, E., Poulain, P. M., Mauri, E., Menna, M., & Notarstefano, G. (2019). Levantine intermediate and Levantine deep water formation: An Argo float study from 2001 to 2017. *Water*, *11*(9), 26. https://doi.org/10.3390/w11091781

Kutzbach, J. E., Chen, G., Cheng, H., Edwards, R. L., & Liu, Z. (2014). Potential role of winter rainfall in explaining increased moisture in the Mediterranean and Middle East during periods of maximum orbitally-forced insolation seasonality. *Climate Dynamics*, *42*(3-4), 1079–1095. https://doi.org/10.1007/s00382-013-1692-1

Lascaratos, A., Williams, R. G., & Tragou, E. (1993). A mixed-layer study of the formation of Levantine intermediate water. *Journal of Geophysical Research*, *98*(C8), 14,739–14,749. https://doi.org/10.1029/93jc00912

Lebreiro, S. M., Antón, L., Reguera, M. I., Fernández, M., Conde, E., Barrado, A. I., & Yllera, A. (2015). Zooming into the Mediterranean Outflow fossil moat during the 1.2–1.8 million years period (Early-Pleistocene)—An approach by radiogenic and stable isotopes. *Global and Planetary Change*, *135*, 104–118. https://doi.org/10.1016/j.gloplacha.2015.10.010

Lebreiro, S. M., Anton, L., Reguera, M. I., & Marzocchi, A. (2018). Paleoceanographic and climatic implications of a new Mediterranean Outflow branch in the southern Gulf of Cadiz. *Quaternary Science Reviews*, *197*, 92–111. https://doi.org/10.1016/j.quascirev.2018.07.036

Legg, S., Briegleb, B., Chang, Y., Chassignet, E. P., Danabasoglu, G., Ezer, T., et al. (2009). Improving oceanic overflow representation in climate models. The Gravity Current Entrainment Climate Process Team. *Bulletin of the American Meteorological Society*, *90*(5), 657–670. https://doi.org/10.1175/2008bams2667.1

Lézine, A.-M., Hély, C., Grenier, C., Braconnot, P., & Krinner, G. (2011). Sahara and Sahel vulnerability to climate changes, lessons from Holocene hydrological data. *Quaternary Science Reviews*, *30*(21), 3001–3012. https://doi.org/10.1016/j.quascirev.2011.07.006

Litt, T., Pickarski, N., Heumann, G., Stockhecke, M., & Tzedakis, P. C. (2014). A 600,000 year long continental pollen record from Lake Van, eastern Anatolia (Turkey). *Quaternary Science Reviews*, *104*, 30–41. https://doi.org/10.1016/j.quascirev.2014.03.017

Llave, E., Hernández-Molina, F. J., Somoza, L., Díaz-del-Río, V., Stow, D. A. V., Maestro, A., & Dias, J. A. (2001). Seismic stacking pattern of the Faro-Albufeira contourite system (Gulf of Cadiz): A Quaternary record of paleoceanographic and tectonic influences. *Marine Geophysical Researches*, *22*(5-6), 487–508. https://doi.org/10.1023/A:1016355801344

Llave, E., Hernandez-Molina, F. J., Somoza, L., Stow, D. A. V., & del Rio, V. D. (2007). Quaternary evolution of the contourite depositional system in the Gulf of Cadiz. In A. R. Viana, & M. Rebesco (Eds.), *Economic and palaeoceanographic significance of contourite deposits* (Vol. 276, pp. 49–79). Bath: Geological Soc Publishing House.

Llave, E., Schönfeld, J., Hernández-Molina, F. J., Mulder, T., Somoza, L., Del Río, V. D., & Sánchez-Almazo, I. (2006). High-resolution stratigraphy of the Mediterranean Outflow contourite system in the Gulf of Cadiz during the late Pleistocene: The impact of Heinrich events. *Marine Geology*, *227*(3-4), 241–262. https://doi.org/10.1016/j.margeo.2005.11.015

Lofi, J., Voelker, A. H. L., Ducassou, E., Hernández-Molina, F. J., Sierro, F. J., Bahr, A., et al. (2016). Quaternary chronostratigraphic framework and sedimentary processes for the Gulf of Cadiz and Portuguese contourite depositional systems derived from natural gamma ray records. *Marine Geology*, *377*, 40–57. https://doi.org/10.1016/j.margeo.2015.12.005

Magill, C. R., Ausín, B., Wenk, P., McIntyre, C., Skinner, L., Martínez-García, A., et al. (2018). Transient hydrodynamic effects influence organic carbon signatures in marine sediments. *Nature Communications*, *9*, 8. https://doi.org/10.1038/s41467-018-06973-w

Magri, D., & Tzedakis, P. C. (2000). Orbital signatures and long-term vegetation patterns in the Mediterranean. *Quaternary International*, *73-4*, 69–78. https://doi.org/10.1016/s1040-6182(00)00065-3

Major, C., Ryan, W., Lericolais, G., & Hajdas, I. (2002). Constraints on Black Sea outflow to the Sea of Marmara during the last glacial-interglacial transition. *Marine Geology*, *190*(1-2), 19–34. https://doi.org/10.1016/s0025-3227(02)00340-7

Major, C. O., Goldstein, S. L., Ryan, W. B. F., Lericolais, G., Piotrowski, A. M., & Hajdas, I. (2006). The co-evolution of Black Sea level and composition through the last deglaciation and its paleoclimatic significance. *Quaternary Science Reviews*, *25*(17-18), 2031–2047. https://doi.org/10.1016/j.quascirev.2006.01.032

Marino, G., Rohling, E. J., Rodríguez-Sanz, L., Grant, K. M., Heslop, D., Roberts, A. P., et al. (2015). Bipolar seesaw control on last interglacial sea level. *Nature*, *522*(7555), 197–201. https://doi.org/10.1038/nature14499

Martinez-Lamas, R., Toucanne, S., Debret, M., Riboulot, V., Deloffre, J., Boissier, A., et al. (2020). Linking Danube River activity to Alpine Ice-Sheet fluctuations during the last glacial (ca. 33–17 ka BP): Insights into the continental signature of Heinrich stadials. *Quaternary Science Reviews*, *229*, 106,136. https://doi.org/10.1016/j.quascirev.2019.106136

Martin-Garcia, G. M., Alonso-Garcia, M., Sierro, F. J., Hodell, D. A., & Flores, J. A. (2015). Severe cooling episodes at the onset of deglaciations on the southwestern Iberian Margin from MIS 21 to 13 (IODP Site U1385). *Global and Planetary Change*, *135*, 159–169. https://doi.org/10.1016/j.gloplacha.2015.11.001

Martins, V. A., Santos, J. F., Mackensen, A., Dias, J. A., Ribeiro, S., Moreno, J. C., et al. (2013). The sources of the glacial IRD in the NW Iberian Continental Margin over the last 40 ka. *Quaternary International*, *318*, 128–138. https://doi.org/10.1016/j.quaint.2013.08.026

Martrat, B., Grimalt, J. O., Lopez-Martinez, C., Cacho, I., Sierro, F. J., Flores, J. A., et al. (2004). Abrupt temperature changes in the Western Mediterranean over the past 250,000 years. *Science*, *306*(5702), 1762–1765. https://doi.org/10.1126/science.1101706

Martrat, B., Grimalt, J. O., Shackleton, N. J., de Abreu, L., Hutterli, M. A., & Stocker, T. F. (2007). Four climate cycles of recurring deep and surface water destabilizations on the Iberian margin. *Science*, *317*(5837), 502–507. https://doi.org/10.1126/science.1139994

Martrat, B., Jimenez-Amat, P., Zahn, R., & Grimalt, J. O. (2014). Similarities and dissimilarities between the last two deglaciations and interglaciations in the North Atlantic region. *Quaternary Science Reviews*, *99*, 122–134. https://doi.org/10.1016/j.quascirev.2014.06.016

Marzocchi, A., Flecker, R., Lunt, D. J., Krijgsman, W., & Hilgen, F. J. (2019). Precessional drivers of late Miocene Mediterranean sedimentary sequences: African summer monsoon and Atlantic winter storm tracks. *Paleoceanography and Paleoclimatology*, *34*(12), 1980–1994. https://doi.org/10.1029/2019PA003721

Mauritzen, C., Morel, Y., & Paillet, J. (2001). On the influence of Mediterranean water on the central waters of the North Atlantic Ocean. *Deep-Sea Research Part I: Oceanographic Research Papers*, *48*(2), 347–381. https://doi.org/10.1016/S0967-0637(00)00043-1

McCave, I. N., Manighetti, B., & Robinson, S. G. (1995). Sortable silt and fine sediment size/composition slicing: Parameters for palaeocurrent speed and palaeoceanography. *Paleoceanography*, *10*(3), 593–610. https://doi.org/10.1029/94PA03039

McManus, J. F., Francois, R., Gherardi, J. M., Keigwin, L. D., & Brown-Leger, S. (2004). Collapse and rapid resumption of Atlantic meridional circulation linked to deglacial climate changes. *Nature*, *428*(6985), 834–837. https://doi.org/10.1038/nature02494

Ménot, G., Bard, E., Rostek, F., Weijers, J. W., Hopmans, E. C., Schouten, S., & Damsté, J. S. S. (2006). Early reactivation of European rivers during the last deglaciation. *Science*, *313*(5793), 1623–1625. https://doi.org/10.1126/science.1130511

Millot, C. (1999). Circulation in the western Mediterranean Sea. *Journal of Marine Systems*, *20*(1-4), 423–442. https://doi.org/10.1016/s0924-7963(98)00078-5

Millot, C. (2013). Levantine intermediate water characteristics: An astounding general misunderstanding! *Scientia Marina*, *77*(2), 217–232. https://doi.org/10.3989/scimar.03518.13A

Millot, C. (2014). Heterogeneities of in- and out-flows in the Mediterranean Sea. *Progress in Oceanography*, *120*, 254–278. https://doi.org/10.1016/j.pocean.2013.09.007

Millot, C., Candela, J., Fuda, J. L., & Tber, Y. (2006). Large warming and salinification of the Mediterranean Outflow due to changes in its composition. *Deep-Sea Research Part I-Oceanographic Research Papers*, *53*(4), 656–666. https://doi.org/10.1016/j.dsr.2005.12.017

Minto'o, C. A., Bassetti, M. A., Morigi, C., Ducassou, E., Toucanne, S., Jouet, G., & Mulder, T. (2015). Levantine intermediate water hydrodynamic and bottom water ventilation in the northern Tyrrhenian Sea over the past 56,000 years: New insights from benthic foraminifera and ostracods. *Quaternary International*, *357*, 295–313. https://doi.org/10.1016/j.quaint.2014.11.038

Mojtahid, M., Toucanne, S., Fentimen, R., Barras, C., Le Houedec, S., Soulet, G., et al. (2017). Changes in northeast Atlantic hydrology during Termination 1: Insights from Celtic margin's benthic foraminifera. *Quaternary Science Reviews*, *175*, 45–59. https://doi.org/10.1016/j.quascirev.2017.09.003

Monegato, G., Scardia, G., Hajdas, I., Rizzini, F., & Piccin, A. (2017). The Alpine LGM in the boreal ice-sheets game. *Scientific Reports*, *7*. https://doi.org/10.1038/s41598-017-02148-7

Mulder, T., Hassan, R., Ducassou, E., Zaragosi, S., Gonthier, E., Hanquiez, V., et al. (2013). Contourites in the Gulf of Cadiz: A cautionary note on potentially ambiguous indicators of bottom current velocity. *Geo-Marine Letters*, *33*(5), 357–367.

Nelson, C. H., Baraza, J., & Maldonado, A. (1993). Mediterranean Undercurrent sandy contourites, gulf of Cadiz, Spain. *Sedimentary Geology*, *82*(1-4), 103-131. https://doi.org/10.1016/0037-0738(93)90116-M

Ng, H. C., Robinson, L. F., McManus, J. F., Mohamed, K. J., Jacobel, A. W., Ivanovic, R. F., et al. (2018). Coherent deglacial changes in western Atlantic Ocean circulation. *Nature Communications*, *9*(1), 1–10. https://doi.org/10.1038/s41467-018-05312-3

North Greenland Ice Core Project members (2004). High-resolution record of Northern Hemisphere climate extending into the last interglacial period. *Nature*, *431*, 147–151.

Oppo, D. W., McManus, J. F., & Cullen, J. L. (2006). Evolution and demise of the Last Interglacial warmth in the subpolar North Atlantic. *Quaternary Science Reviews*, *25*(23-24), 3268–3277. https://doi.org/10.1016/j.quascirev.2006.07.006

Ozgokmen, T. M., Chassignet, E. P., & Rooth, C. G. H. (2001). On the connection between the Mediterranean Outflow and the Azores Current. *Journal of Physical Oceanography, 31*(2), 461-480. https://doi.org/10.1175/1520-0485(2001)031<0461:otcbtm>2.0.co;2

Pahnke, K., Goldstein, S. L., & Hemming, S. R. (2008). Abrupt changes in Antarctic intermediate water circulation over the past 25,000 years. *Nature Geoscience*, *1*(12), 870–874. https://doi.org/10.1038/ngeo360

Peck, V. L., Hall, I. R., Zahn, R., Elderfield, H., Grousset, F., Hemming, S. R., & Scourse, J. D. (2006). High resolution evidence for linkages between NW European ice sheet instability and Atlantic Meridional Overturning Circulation. *Earth and Planetary Science Letters*, *243*(3-4), 476–488. https://doi.org/10.1016/epsl.2005.12.023

Peck, V. L., Hall, I. R., Zahn, R., Grousset, F., Hemming, S. R., & Scourse, J. D. (2007). The relationship of Heinrich events and their European precursors over the past 60 ka BP: A multi-proxy ice-rafted debris provenance study in the north East Atlantic. *Quaternary Science Reviews*, *26*(7-8), 862–875. https://doi.org/10.1016/j.quascirev.2006.12.002

Peck, V. L., Hall, I. R., Zahn, R., & Scourse, J. D. (2007). Progressive reduction in NE Atlantic intermediate water ventilation prior to Heinrich events: Response to NW European ice sheet instabilities? *Geochemistry Geophysics Geosystems*, *8*. https://doi.org/10.1029/2006gc001321

Peliz, A., Dubert, J., Santos, A. M. P., Oliveira, P. B., & Le Cann, B. (2005). Winter upper ocean circulation in the western Iberian Basin—Fronts, eddies and poleward flows: An overview. *Deep-Sea Research Part I-Oceanographic Research Papers*, *52*(4), 621–646. https://doi.org/10.1016/j.dsr.2004.11.005

Peliz, A., Marchesiello, P., Santos, A. M. P., Dubert, J., Teles-Machado, A., Marta-Almeida, M., & Le Cann, B. (2009). Surface circulation in the Gulf of Cadiz: 2. Inflow-outflow coupling and the Gulf of Cadiz slope current. *Journal of Geophysical Research*, *114*. https://doi.org/10.1029/2008jc004771

Perez-Folgado, M., Sierro, F. J., Flores, J. A., Grimalth, J. O., & Zahn, R. (2004). Paleoclimatic variations in foraminifer assemblages from the Alboran Sea (western Mediterranean) during the last 150 ka in ODP Site 977. *Marine Geology*, *212*(1-4), 113–131. https://doi.org/10.1016/j.margeo.2004.08.002

Pinardi, N., Cessi, P., Borile, F., & Wolfe, C. L. P. (2019). The Mediterranean Sea overturning circulation. *Journal of Physical Oceanography*, *49*(7), 1699–1721. https://doi.org/10.1175/jpo-d-18-0254.1

Pinardi, N., & Masetti, E. (2000). Variability of the large scale general circulation of the Mediterranean Sea from observations and modelling: A review. *Palaeogeography Palaeoclimatology Palaeoecology*, *158*(3-4), 153–174. https://doi.org/10.1016/s0031-0182(00)00048-1

Plaza-Morlote, M., Rey, D., Santos, J. F., Ribeiro, S., Heslop, D., Bernabeu, A., et al. (2017). Southernmost evidence of large European Ice Sheet-derived freshwater discharges during the Heinrich Stadials of the Last Glacial Period (Galician Interior Basin, northwest Iberian Continental Margin). *Earth and Planetary Science Letters*, *457*, 213–226. https://doi.org/10.1016/j.epsl.2016.10.020

Price, J. F., Baringer, M. O. N., Lueck, R. G., Johnson, G. C., Ambar, I., Parrilla, G., et al. (1993). Mediterranean Outflow mixing and dynamics. *Science*, *259*(5099), 1277–1282. https://doi.org/10.1126/science.259.5099.1277

Racape, V., Thierry, V., Mercier, H., & Cabanes, C. (2019). ISOW spreading and mixing as revealed by Deep-Argo floats launched in the Charlie-Gibbs fracture zone. *Journal of Geophysical Research: Oceans*, *124*, 6787–6808. https://doi.org/10.1029/2019jc015040

Rahmstorf, S. (1998). Influence of Mediterranean Outflow on climate. *Eos, Transactions American Geophysical Union*, *79*(24), 281–282. https://doi.org/10.1029/98EO00208

Railsback, L. B., Gibbard, P. L., Head, M. J., Voarintsoa, N. R. G., & Toucanne, S. (2015). An optimized scheme of lettered marine isotope substages for the last 1.0 million years, and the climatostratigraphic nature of isotope stages and substages. *Quaternary Science Reviews*, *111*, 94–106.

Rasmussen, S. O., Bigler, M., Blockley, S. P., Blunier, T., Buchardt, S. L., Clausen, H. B., et al. (2014). A stratigraphic framework for abrupt climatic changes during the Last Glacial period based on three synchronized Greenland ice-core records: Refining and extending the INTIMATE event stratigraphy. *Quaternary Science Reviews*, *106*, 14–28.

Ravazzi, C., Pini, R., Badino, F., De Amicis, M., Londeix, L., & Reimer, P. J. (2014). The latest LGM culmination of the Garda Glacier (Italian Alps) and the onset of glacial termination. Age of glacial collapse and vegetation chronosequence. *Quaternary Science Reviews*, *105*, 26–47. https://doi.org/10.1016/j.quascirev.2014.09.014

Reid, J. L. (1979). Contribution of the Mediterranean-sea Outflow to the Norwegian Greenland Sea. *Deep-Sea Research Part A-Oceanographic Research Papers*, *26*(11), 1199–1223. https://doi.org/10.1016/0198-0149(79)90064-5

Revel, M., Ducassou, E., Grousset, F. E., Bernasconi, S. M., Migeon, S., Révillon, S., et al. (2010). 100,000 years of African monsoon variability recorded in sediments of the Nile margin. *Quaternary Science Reviews*, *29*(11-12), 1342–1362. https://doi.org/10.1016/j.quascirev.2010.02.006

Rickaby, R. E. M., & Elderfield, H. (2005). Evidence from the high-latitude North Atlantic for variations in Antarctic intermediate water flow during the last deglaciation. *Geochemistry Geophysics Geosystems*, *6*, 12. https://doi.org/10.1029/2004gc000858

Roberts, D. H., Long, A. J., Schnabel, C., Freeman, S., & Simpson, M. J. R. (2008). The deglacial history of southeast sector of the Greenland Ice Sheet during the Last Glacial Maximum. *Quaternary Science Reviews*, *27*(15-16), 1505–1516. https://doi.org/10.1016/j.quascirev.2008.04.008

Roether, W., Manca, B. B., Klein, B., Bregant, D., Georgopoulos, D., Beitzel, V., et al. (1996). Recent changes in eastern Mediterranean deep waters. *Science*, *271*(5247), 333–335. https://doi.org/10.1126/science.271.5247.333

Roether, W., & Schlitzer, R. (1991). Eastern Mediterranean deep-water renewal on the basis of chlorofluoromethane and tritium data. *Dynamics of Atmospheres and Oceans*, *15*(3-5), 333–354. https://doi.org/10.1016/0377-0265(91)90025-b

Rogerson, M., Bigg, G. R., Rohling, E. J., & Ramirez, J. (2012). Vertical density gradient in the eastern North Atlantic during the last 30,000 years. *Climate Dynamics*, *39*(3-4), 589–598. https://doi.org/10.1007/s00382-011-1148-4

Rogerson, M., Dublyansky, Y., Hoffmann, D. L., Luetscher, M., Tochterle, P., & Spotl, C. (2019). Enhanced Mediterranean water cycle explains increased humidity during MIS 3 in North Africa. *Climate of the Past*, *15*(5), 1757–1769. https://doi.org/10.5194/cp-15-1757-2019

Rogerson, M., Rohling, E. J., Bigg, G. R., & Ramirez, J. (2012). Paleoceanography of the Atlantic-Mediterranean exchange: Overview and first quantitative assessment of climatic forcing. *Reviews of Geophysics*, *50*, RG2003. https://doi.org/10.1029/2011rg000376

Rogerson, M., Rohling, E. J., & Weaver, P. P. E. (2006). Promotion of meridional overturning by Mediterranean-derived salt during the last deglaciation. *Paleoceanography*, *21*, PA4101. https://doi.org/10.1029/2006pa001306

Rogerson, M., Rohling, E. J., Weaver, P. P. E., & Murray, J. W. (2005). Glacial to interglacial changes in the settling depth of the Mediterranean Outflow plume. *Paleoceanography*, *20*, PA3007. https://doi.org/10.1029/2004pa001106

Rohling, E. J., & Hilgen, F. J. (1991). The eastern Mediterranean climate at times of sapropel formation: A review. *Geologie en Mijnbouw*, *70*(3), 253–264.

Rohling, E. J., Marino, G., & Grant, K. M. (2015). Mediterranean climate and oceanography, and the periodic development of anoxic events (sapropels). *Earth-Science Reviews*, *143*, 62–97. https://doi.org/10.1016/j.earscirev.2015.01.008

Roque, D., Parras-Berrocal, I., Bruno, M., Sanchez-Leal, R., & Hernandez-Molina, F. J. (2019). Seasonal variability of intermediate water masses in the Gulf of Cadiz: Implications of the Antarctic and subarctic seesaw. *Ocean Science*, *15*(5), 1381–1397. https://doi.org/10.5194/os-15-1381-2019

Rossignol-Strick, M., Nesteroff, W., Olive, P., & Vergnaud-Grazzini, C. (1982). After the deluge: Mediterranean stagnation and sapropel formation. *Nature*, *295*(5845), 105–110. https://doi.org/10.1038/295105a0

Ryan, W. B. F., Major, C. O., Lericolais, G., & Goldstein, S. L. (2003). Catastrophic flooding of the Black Sea. *Annual Review of Earth and Planetary Sciences*, *31*, 525–554. https://doi.org/10.1146/annurev.earth.31.100901.141249

Sancez Goñi, M., Cacho, I., Turon, J. L., Guiot, J., Sierro, F. J., Peypouquet, J. P., et al. (2002). Synchroneity between marine and terrestrial responses to millennial scale climatic variability during the last glacial period in the Mediterranean region. *Climate Dynamics*, *19*(1), 95–105. https://doi.org/10.1007/s00382-001-0212-x

Sanchez-Leal, R. F., Bellanco, M. J., Fernandez-Salas, L. M., Garcia-Lafuente, J., Gasser-Rubinat, M., Gonzalez-Pola, C., et al. (2017). The Mediterranean Overflow in the Gulf of Cadiz: A Rugged Journey. *Science Advances, 3*(11), eaao0609-eaao0609. https://doi.org/10.1126/sciadv.aao0609

Schonfeld, J., & Zahn, R. (2000). Late Glacial to Holocene history of the Mediterranean Outflow. Evidence from benthic foraminiferal assemblages and stable isotopes at the Portuguese margin. *Palaeogeography Palaeoclimatology Palaeoecology*, *159*(1-2), 85–111. https://doi.org/10.1016/s0031-0182(00)00035-3

Schonfeld, J., Zahn, R., & de Abreu, L. (2003). Surface and deep water response to rapid climate changes at the western Iberian Margin. *Global and Planetary Change*, *36*(4), 237–264. https://doi.org/10.1016/s0921-8181(02)00197-2

Schott, F., Visbeck, M., Send, U., Fischer, J., Stramma, L., & Desaubies, Y. (1996). Observations of deep convection in the Gulf of Lions, northern Mediterranean, during the winter of 1991/92. *Journal of Physical Oceanography, 26*(4), 505-524. https://doi.org/10.1175/1520-0485(1996)026<0505:OODCIT>2.0.CO;2

Schroeder, K., Ribotti, A., Borghini, M., Sorgente, R., Perilli, A., & Gasparini, G. P. (2008). An extensive western Mediterranean deep water renewal between 2004 and 2006. *Geophysical Research Letters*, *35*, L18605. https://doi.org/10.1029/2008gl035146

Shakun, J. D., Burns, S. J., Fleitmann, D., Kramers, J., Matter, A., & Al-Subary, A. (2007). A high-resolution, absolute-dated deglacial speleothem record of Indian Ocean climate from Socotra Island, Yemen. *Earth and Planetary Science Letters*, *259*(3-4), 442–456. https://doi.org/10.1016/j.epsl.2007.05.004

Shanahan, T. M., McKay, N. P., Hughen, K. A., Overpeck, J. T., Otto-Bliesner, B., Heil, C. W., et al. (2015). The time-transgressive termination of the African humid period. *Nature Geosci*, *8*(2), 140–144. https://doi.org/10.1038/ngeo2329

Sierro, F., Flores, J., & Baraza, J. (1999). Late glacial to recent paleoenvironmental changes in the Gulf of Cadiz and formation of sandy contourite layers. *Marine Geology, 155*(1-2), 157-172. https://doi.org/10.1016/S0025-3227(98)00145-5

Sierro, F. J., Hodell, D. A., Curtis, J. H., Flores, J. A., Reguera, I., Colmenero-Hidalgo, E., et al. (2005). Impact of iceberg melting on Mediterranean thermohaline circulation during Heinrich events. *Paleoceanography*, *20*, PA2019. https://doi.org/10.1029/2004pa001051

Singh, A. D., Rai, A. K., Tiwari, M., Naidu, P. D., Verma, K., Chaturvedi, M., et al. (2015). Fluctuations of Mediterranean Outflow water circulation in the Gulf of Cadiz during MIS 5 to 7: Evidence from benthic foraminiferal assemblage and stable isotope records. *Global and Planetary Change*, *133*, 125–140. https://doi.org/10.1016/j.gloplacha.2015.08.005

Skinner, L. C., & Shackleton, N. J. (2006). Deconstructing Terminations I and II: Revisiting the glacioeustatic paradigm based on deep-water temperature estimates. *Quaternary Science Reviews*, *25*(23-24), 3312–3321. https://doi.org/10.1016/j.quascirev.2006.07.005

Skinner, L. C., Shackleton, N. J., & Elderfield, H. (2003). Millennial-scale variability of deep-water temperature and delta O-18(dw) indicating deep-water source variations in the Northeast Atlantic, 0-34 cal. ka BP. *Geochemistry Geophysics Geosystems*, *4*. https://doi.org/10.1029/2003gc000585

Skliris, N., Sofianos, S., & Lascaratos, A. (2007). Hydrological changes in the Mediterranean Sea in relation to changes in the freshwater budget: A numerical modelling study. *Journal of Marine Systems*, *65*(1-4), 400–416. https://doi.org/10.1016/j.jmarsys.2006.01.015

Soto-Navarro, J., Criado-Aldeanueva, F., Sanchez-Garrido, J. C., & Garcia-Lafuente, J. (2012). Recent thermohaline trends of the Atlantic waters inflowing to the Mediterranean Sea. *Geophysical Research Letters*, *39*, L01604. https://doi.org/10.1029/2011gl049907

Soulet, G., Ménot, G., Bayon, G., Rostek, F., Ponzevera, E., Toucanne, S., et al. (2013). Abrupt drainage cycles of the Fennoscandian Ice Sheet. *Proceedings of the National Academy of Sciences of the United States of America*, *110*(17), 6682–6687. https://doi.org/10.1073/pnas.1214676110

Sprovieri, M., Di Stefano, E., Incarbona, A., Manta, D. S., Pelosi, N., d'Alcalà, M. R., & Sprovieri, R. (2012). Centennial- to millennial-scale climate oscillations in the central-eastern Mediterranean Sea between 20,000 and 70,000 years ago: Evidence from a high-resolution geochemical and micropaleontological record. *Quaternary Science Reviews*, *46*, 126–135. https://doi.org/10.1016/j.quascirev.2012.05.005

Stanford, J. D., Rohling, E. J., Bacon, S., Roberts, A. P., Grousset, F. E., & Bolshaw, M. (2011). A new concept for the paleoceanographic evolution of Heinrich Event 1 in the North Atlantic. *Quaternary Science Reviews*, *30*(9-10), 1047–1066. https://doi.org/10.1016/j.quascirev.2011.02.003

Stow, D. A., Faugères, J. C., Gonthier, E., Cremer, M., Llave, E., Hernández-Molina, F. J., et al. (2002). Faro-Albufeira drift complex, northern Gulf of Cadiz. *Geological Society, London, Memoirs*, *22*(1), 137–154. https://doi.org/10.1144/GSL.MEM.2002.022.01.11

Stow, D. A. V., Faugeres, J. C., & Gonthier, E. (1986). Facies distribution and textural variation in Faro drift contourites—Velocity fluctuation and drift growth. *Marine Geology*, *72*(1-2), 71–100. https://doi.org/10.1016/0025-3227(86)90100-3

Stow, D. A. V., Hernández-Molina, F. J., Alvarez Zarikian, C. A., & Expedition 339 Scientists (2013). Proceedings of the IODP, 339, Integrated Ocean Drilling Program Management International, Inc., Tokyo. https://doi.org/10.2204/iodp.proc.339.2013

Swingedouw, D., Colin, C., Eynaud, F., Ayache, M., & Zaragosi, S. (2019). Impact of freshwater release in the Mediterranean Sea on the North Atlantic climate. *Climate Dynamics*, *53*(7-8), 3893–3915. https://doi.org/10.1007/s00382-019-04758-5

Thiagarajan, N., Subhas, A. V., Southon, J. R., Eiler, J. M., & Adkins, J. F. (2014). Abrupt pre-Bolling-Allerod warming and circulation changes in the deep ocean. *Nature*, *511*(7507), 75–U409. https://doi.org/10.1038/nature13472

Tombo, S. L., Dennielou, B., Berné, S., Bassetti, M. A., Toucanne, S., Jorry, S. J., et al. (2015). Sea-level control on turbidite activity in the Rhone canyon and the upper fan during the Last Glacial Maximum and early deglacial. *Sedimentary Geology*, *323*, 148–166. https://doi.org/10.1016/j.sedgeo.2015.04.009

Toucanne, S., Jouet, G., Ducassou, E., Bassetti, M. A., Dennielou, B., Minto'o, C. M. A., et al. (2012). A 130,000-year record of Levantine intermediate water flow variability in the Corsica Trough, western Mediterranean Sea. *Quaternary Science Reviews*, *33*, 55–73. https://doi.org/10.1016/j.quascirev.2011.11.020

Toucanne, S., Minto'o, C. M. A., Fontanier, C., Bassetti, M.-A., Jorry, S. J., & Jouet, G. (2015). Tracking rainfall in the northern Mediterranean borderlands during sapropel deposition. *Quaternary Science Reviews*, *129*, 178–195. https://doi.org/10.1016/j.quascirev.2015.10.016

Toucanne, S., Mulder, T., Schönfeld, J., Hanquiez, V., Gonthier, E., Duprat, J., et al. (2007). Contourites of the Gulf of Cadiz: A high-resolution record of the paleocirculation of the Mediterranean Outflow water during the last 50,000 years. *Palaeogeography Palaeoclimatology Palaeoecology*, *246*(2-4), 354–366. https://doi.org/10.1016/j.palaeo.2006.10.007

Toucanne, S., Soulet, G., Freslon, N., Jacinto, R. S., Dennielou, B., Zaragosi, S., et al. (2015). Millennial-scale fluctuations of the European Ice Sheet at the end of the last glacial, and their potential impact on global climate. *Quaternary Science Reviews*, *123*, 113–133. https://doi.org/10.1016/j.quascirev.2015.06.010

Toucanne, S., Zaragosi, S., Bourillet, J. F., Cremer, M., Eynaud, F., Van Vliet-Lanoë, B., et al. (2009). Timing of massive 'Fleuve Manche'discharges over the last 350 kyr: Insights into the European ice-sheet oscillations and the European drainage network from MIS 10 to 2. *Quaternary Science Reviews*, *28*(13-14), 1238–1256. https://doi.org/10.1016/j.quascirev.2009.01.006

Toucanne, S., Zaragosi, S., Bourillet, J. F., Marieu, V., Cremer, M., Kageyama, M., et al. (2010). The first estimation of Fleuve Manche palaeoriver discharge during the last deglaciation: Evidence for Fennoscandian ice sheet meltwater flow in the English Channel ca 20–18 ka ago. *Earth and Planetary Science Letters*, *290*(3), 459–473. https://doi.org/10.1016/j.epsl.2009.12.050

Tripsanas, E. K., Panagiotopoulos, I. P., Lykousis, V., Morfis, I., Karageorgis, A. P., Anastasakis, G., & Kontogonis, G. (2016). Late quaternary bottom-current activity in the south Aegean Sea reflecting climate-driven dense-water production. *Marine Geology*, *375*, 99–119. https://doi.org/10.1016/j.margeo.2015.12.007

Tsimplis, M. N., & Bryden, H. L. (2000). Estimation of the transports through the Strait of Gibraltar. *Deep-Sea Research Part I-Oceanographic Research Papers*, *47*(12), 2219–2242. https://doi.org/10.1016/s0967-0637(00)00024-8

Tudryn, A., Leroy, S. A., Toucanne, S., Gibert-Brunet, E., Tucholka, P., Lavrushin, Y. A., et al. (2016). The Ponto-Caspian basin as a final trap for southeastern Scandinavian Ice-Sheet meltwater. *Quaternary Science Reviews*, *148*, 29–43. https://doi.org/10.1016/j.quascirev.2016.06.019

Tzedakis, P. C. (2005). Towards an understanding of the response of southern European vegetation to orbital and suborbital climate variability. *Quaternary Science Reviews*, *24*(14-15), 1585–1599. https://doi.org/10.1016/j.quascirev.2004.11.012

Tzedakis, P. C., Hooghiemstra, H., & Palike, H. (2006). The last 1.35 million years at Tenaghi Philippon: Revised chronostratigraphy and long-term vegetation trends. *Quaternary Science Reviews*, *25*(23-24), 3416–3430. https://doi.org/10.1016/j.quascirev.2006.09.002

Tzedakis, P. C., Lawson, I. T., Frogley, M. R., Hewitt, G. M., & Preece, R. C. (2002). Buffered tree population changes in a quaternary refugium: Evolutionary implications. *Science*, *297*(5589), 2044–2047. https://doi.org/10.1126/science.1073083

Tzedakis, P. C., Palike, H., Roucoux, K. H., & de Abreu, L. (2009). Atmospheric methane, southern European vegetation and low-mid latitude links on orbital and millennial timescales. *Earth and Planetary Science Letters*, *277*(3-4), 307–317. https://doi.org/10.1016/j.epsl.2008.10.027

van Aken, H. M. (2000). The hydrography of the mid-latitude northeast Atlantic Ocean II: The intermediate water masses. *Deep-Sea Research Part I-Oceanographic Research Papers*, *47*(5), 789–824. https://doi.org/10.1016/s0967-0637(99)00112-0

van Aken, H. M. (2001). The hydrography of the mid-latitude northeast Atlantic Ocean—Part III: The subducted thermocline water mass. *Deep-Sea Research Part I-Oceanographic Research Papers*, *48*(1), 237–267. https://doi.org/10.1016/s0967-0637(00)00059-5

Voelker, A. H., Salgueiro, E., Rodrigues, T., Jimenez-Espejo, F. J., Bahr, A., Alberto, A., et al. (2015). Mediterranean Outflow and surface water variability off southern Portugal during the early Pleistocene: A snapshot at Marine Isotope Stages 29 to 34 (1020–1135 ka). *Global and Planetary Change*, *133*, 223–237. https://doi.org/10.1016/j.gloplacha.2015.08.015

Voelker, A. H. L., Colman, A., Olack, G., Waniek, J. J., & Hodell, D. (2015). Oxygen and hydrogen isotope signatures of northeast Atlantic water masses. Deep Sea Research Part II. *Topical Studies in Oceanography*, *116*, 89–106. https://doi.org/10.1016/j.dsr2.2014.11.006

Voelker, A. H. L., & de Abreu, L. (2011). A review of abrupt climate change events in the northeastern Atlantic Ocean (Iberian Margin): Latitudinal, longitudinal, and vertical gradients. In H. Rashid, L. Polyak, & E. MosleyThompson (Eds.), *Abrupt climate change: Mechanisms, patterns, and impacts* (Vol. 193, pp. 15–37). Washington: Amer Geophysical Union. https://doi.org/10.1029/2010GM001021

Voelker, A. H. L., de Abreu, L., Schönfeld, J., Erlenkeuser, H., & Abrantes, F. (2009). Hydrographic conditions along the western Iberian Margin during marine isotope stage 2. *Geochemistry, Geophysics, Geosystems*, *10*. https://doi.org/10.1029/2009GC002605

Voelker, A. H. L., Lebreiro, S. M., Schonfeld, J., Cacho, I., Erlenkeuser, H., & Abrantes, F. (2006). Mediterranean Outflow strengthening during Northern Hemisphere coolings: A salt source for the glacial Atlantic? *Earth and Planetary Science Letters*, *245*, 39–55. https://doi.org/10.1016/j.epsl.2006.03.014

Volkov, D. L., & Fu, L. L. (2010). On the reasons for the formation and variability of the Azores Current. *Journal of Physical Oceanography*, *40*(10), 2197–2220. https://doi.org/10.1175/2010JPO4326.1

Waelbroeck, C., Skinner, L. C., Labeyrie, L., Duplessy, J. C., Michel, E., Vazquez Riveiros, N., et al. (2011). The timing of deglacial circulation changes in the Atlantic. *Paleoceanography*, *26*. https://doi.org/10.1029/2010pa002007

Wagner, B., Vogel, H., Francke, A., Friedrich, T., Donders, T., Lacey, J. H., et al. (2019). Mediterranean winter rainfall in phase with African monsoons during the past 1.36 million years. *Nature*, *573*(7773), 256–260. https://doi.org/10.1038/s41586-019-1529-0

Wang, Y. J., Cheng, H., Edwards, R. L., An, Z. S., Wu, J. Y., Shen, C. C., & Dorale, J. A. (2001). A high-resolution absolute-dated Late Pleistocene monsoon record from Hulu Cave, China. *Science*, *294*(5550), 2345–2348. https://doi.org/10.1126/science.1064618

Willamowski, C., & Zahn, R. (2000). Upper ocean circulation in the glacial North Atlantic from benthic foraminiferal isotope and trace element fingerprinting. *Paleoceanography*, *15*(5), 515–527. https://doi.org/10.1029/1999pa000467

Yasuhara, M., DeMenocal, P. B., Dwyer, G. S., Cronin, T. M., Okahashi, H., & Huang, H. H. M. (2019). North Atlantic intermediate water variability over the past 20,000 years. *Geology*, *47*(7), 659–663. https://doi.org/10.1130/g46161.1

Zahn, R., Schonfeld, J., Kudrass, H. R., Park, M. H., Erlenkeuser, H., & Grootes, P. (1997). Thermohaline instability in the North Atlantic during meltwater events: Stable isotope and ice-rafted detritus records from core SO75-26KL, Portuguese margin. *Paleoceanography*, *12*(5), 696–710. https://doi.org/10.1029/97pa00581

Zahn, R., & Stuber, A. (2002). Suborbital intermediate water variability inferred from paired benthic foraminiferal Cd/Ca and delta C-13 in the tropical West Atlantic and linking with North Atlantic climates. *Earth and Planetary Science Letters*, *200*(1-2), 191–205. https://doi.org/10.1016/s0012-821x(02)00613-1

Zanchetta, G., Drysdale, R. N., Hellstrom, J. C., Fallick, A. E., Isola, I., Gagan, M. K., & Pareschi, M. T. (2007). Enhanced rainfall in the western Mediterranean during deposition of sapropel S1: Stalagmite evidence from Corchia cave (Central Italy). *Quaternary Science Reviews*, *26*(3-4), 279–286. https://doi.org/10.1016/j.quascirev.2006.12.003

Zaragosi, S., Bourillet, J. F., Eynaud, F., Toucanne, S., Denhard, B., Van Toer, A., & Lanfumey, V. (2006). The impact of the last European deglaciation on the deep-sea turbidite systems of the Celtic-Armorican margin (Bay of Biscay). *Geo-Marine Letters*, *26*(6), 317–329. https://doi.org/10.1007/s00367-006-0048-9

Zaragosi, S., Eynaud, F., Pujol, C., Auffret, G. A., Turon, J. L., & Garlan, T. (2001). Initiation of the European deglaciation as recorded in the northwestern Bay of Biscay slope environments (Meriadzek Terrace and Trevelyan Escarpment): A multi-proxy approach. *Earth and Planetary Science Letters*, *188*(3-4), 493–507. https://doi.org/10.1016/s0012-821x(01)00332-6

Ziegler, M., Jilbert, T., de Lange, G. J., Lourens, L. J., & Reichart, G. J. (2008). Bromine counts from XRF scanning as an estimate of the marine organic carbon content of sediment cores. *Geochemistry Geophysics Geosystems*, *9*. https://doi.org/10.1029/2007gc001932

Ziegler, M., Tuenter, E., & Lourens, L. J. (2010). The precession phase of the boreal summer monsoon as viewed from the eastern Mediterranean (ODP Site 968). *Quaternary Science Reviews*, *29*(11-12), 1481–1490. https://doi.org/10.1016/j.quascirev.2010.03.011